Mechanism of Specific Membrane Targeting by C2 Domains: Localized Pools of Target Lipids Enhance Ca^{2+} Affinity†

John A. Corbin,‡ John H. Evans, Kyle E. Landgraf, and Joseph J. Falke*

Molecular Biophysics Program, and Department of Chemistry and Biochemistry, University of Colorado, Boulder, Colorado 80309-0215

Received October 13, 2006; Revised Manuscript Received December 18, 2006

ABSTRACT: The C2 domain is a ubiquitous, conserved protein signaling motif widely found in eukaryotic signaling proteins. Although considerable functional diversity exists, most C2 domains are activated by Ca^{2+} binding and then dock to a specific cellular membrane. The C2 domains of protein kinase Cα (PKCα) and cytosolic phospholipase A_2α (cPLA$_2$α), for example, are known to dock to different membrane surfaces during an intracellular Ca^{2+} signal. Ca^{2+} activation targets the PKCα C2 domain to the plasma membrane and the cPLA$_2$α C2 domain to the internal membranes, with no detectable spatial overlap. It is crucial to determine how such targeting specificity is achieved at physiological bulk Ca^{2+} concentrations that during a typical signaling event rarely exceed 1 μM. For the isolated PKCα C2 domain in the presence of physiological Ca^{2+} levels, the target lipids phosphatidylserine (PS) and phosphatidylinositol-4,5-bisphosphate (PIP_2) are together sufficient to recruit the PKCα C2 domain to a lipid mixture mimicking the plasma membrane inner leaflet. For the cPLA$_2$α C2 domain, the target lipid phosphatidylcholine (PC) appears to be sufficient to drive membrane targeting to an internal membrane mimic at physiological Ca^{2+} levels, although the results do not rule out a second, unknown target molecule. Stopped-flow kinetic studies provide additional information about the fundamental molecular events that occur during Ca^{2+}-activated membrane docking. In principle, C2 domain-directed intracellular targeting, which requires coincidence detection of multiple signals (Ca^{2+} and one or more target lipids), can exhibit two different mechanisms: messenger-activated target affinity (MATA) and target-activated messenger affinity (TAMA). The C2 domains studied here both utilize the TAMA mechanism, in which the C2 domain Ca^{2+} affinity is too low to be activated by physiological Ca^{2+} signals in most regions of the cell. Only when the C2 domain nears its target membrane, which provides a high local concentration of target lipid, is the effective Ca^{2+} affinity increased by the coupled binding equilibrium to a level that enables substantial Ca^{2+} activation and target docking. Overall, the findings emphasize the importance of using physiological ligand concentrations in targeting studies because super-physiological concentrations can drive docking interactions even when an important targeting molecule is missing.

Many signaling pathways are regulated by signaling lipids, membrane proteins, or membrane-bound complexes associated with the plasma or internal cell membranes. Such membrane-associated signaling components control essential processes, such as cellular movement, growth, gene regulation, metabolism, hormone release, and inflammation. One of the most common regulatory elements in membrane-associated signaling pathways is the C2 domain, a ubiquitous, conserved signaling motif recognized in over 200 mammalian proteins (*1*). Structurally, the C2 domain motif comprises eight antiparallel β-strands assembled in a β-sandwich architecture (*2*−*5*). Functionally, although diversity exists (*6*), the C2 motif typically serves as a reversible membrane-targeting element activated by the binding of multiple Ca^{2+} ions (*2*−*5*, *7*, *8*). During a cytoplasmic Ca^{2+} signal, freely diffusing C2 proteins are activated by Ca^{2+} and then dock to specific cellular membranes. The resulting association brings the signaling domains of these proteins to the appropriate target membrane surface, thereby greatly facilitating interactions with membrane-bound substrates or effectors during the duration of the Ca^{2+} signal. Clearly, the ability of a C2 domain to preferentially dock to a specific membrane plays a central role in its function as a targeting element; thus, it is important to understand the molecular mechanisms underlying target-membrane recognition and docking.

Two representative C2 domains, those of protein kinase Cα and cytosolic phospholipase A_2α, have been shown to be useful in comparative studies of membrane-targeting mechanisms (*7*, *9*−*14*). These two well-characterized domains target to mutually exclusive intracellular membrane targets, and their structures (*15*−*19*) and functions (*20*−*22*) are well-studied. More generally, these two domains are representative of broader classes of C2 domains that dock to plasma or internal membranes, respectively, where they carry out essential regulatory functions. The goal of the present study is to elucidate the molecular mechanisms by

† Financial support was provided by NIH Grant GM R01-063235.

* To whom correspondence should be addressed. Tel: 303-492-3597. Fax: 303-492-5894. E-mail: falke@colorado.edu.

‡ Current address: XOMA, LLC, 2910 Seventh Street, Berkeley, CA 94710.

10.1021/bi062140c CCC: $37.00
Published on Web 03/17/2007

which these two C2 domains are recruited specifically to their target membranes, thereby bringing the other domains of their parent proteins into the vicinity of membrane-associated protein or lipid targets.

Protein kinase C isoform α (PKCα[1]) is a ubiquitous signaling protein and a member of the conventional protein kinase C subfamily of serine/threonine kinases (*5*, *22*). The PKCα enzyme regulates a wide array of important pathways ranging from cellular taxis to growth and transformation. The C2 domain of PKCα is an independent folding domain that binds two Ca^{2+} ions (*19*) and drives docking to the plasma membrane, where it recognizes both phosphatidylserine (PS) and phosphatidylinositol-4,5-bisphosphate (PIP_2) as lipid targets (*12*, *23*−*28*). These target lipids bind to two C2 domain sites: PS associates with the two Ca^{2+} ions and nearby amino acids in the Ca^{2+} binding site formed by three inter-strand loops (*19*), whereas PIP_2 binds at a distinct site dominated by side chains on the $\beta3-\beta4$ hairpin (*24*−*28*). When docked to the membrane, the C2 domain contacts the headgroup region of the bilayer in a geometry that enables both of these sites to simultaneously contact their target lipid headgroups (*29*, *30*). The resulting Ca^{2+}-triggered recruitment tethers the C2 domain to the membrane, while another domain, C1, searches for rare, membrane-embedded diacylglycerol molecules that further stabilize the membrane-bound state (*31*, *32*). It is this active, membrane-bound form of PKCα that phosphorylates an array of plasma membrane proteins. Potential targets of PKCα and other conventional PKC isozymes include MARCKS, Raf, coronin, gravin, Ca^{2+} channels, GTPase regulatory proteins, cytoskeletal proteins, and caveolar proteins (*33*−*39*). As observed for other conventional PKC isozymes (*23*, *32*, *40*−*42*), the C2 domain of PKCα is the primary driving force underlying Ca^{2+}-regulated membrane docking such that the isolated C2 domain exhibits the same plasma membrane distribution during an intracellular Ca^{2+} signal as that of the full length protein (*13*). Thus, the isolated C2 domain is fully functional in targeting, and its mechanism of membrane specificity can be studied independent of the other protein domains.

Cytosolic phospholipase A_2 isoform α ($cPLA_2\alpha$) is a ubiquitous signaling protein that hydrolyzes specific phospholipids to release arachidonic acid, a biosynthetic precursor of prostaglandins and leukotrienes that serve as inflammatory agents and chemoattractants (*43*, *44*). The C2 domain of $cPLA_2\alpha$ folds independently and is coupled to the catalytic domain by a long, flexible linker (*18*). During a cytoplasmic Ca^{2+} signal, the C2 domain binds two Ca^{2+} ions (*45*) and docks to intracellular membranes, primarily nuclear, Golgi, and endoplasmic reticulum membranes, where lipids containing arachidonate in the *sn*-2 position are found in highest abundance (*12*, *13*, *46*). The membrane-docked C2 domain is oriented with its three Ca^{2+}-binding loops penetrating into the membrane, where they contact the target lipid phosphatidylcholine (PC) in the headgroup layer and also penetrate more deeply into the hydrocarbon core (*47*−*50*). The docking of the C2 domain to the membrane tethers the catalytic domain in the vicinity of the membrane surface, greatly facilitating its search for substrate lipid molecules. When the C2 and catalytic domains are separated, they retain their distinct targeting and enzymatic functions, respectively (*20*). The isolated C2 domain exhibits the same intracellular membrane distribution during a cytoplasmic Ca^{2+} signal as that of the full length protein (*51*). Thus, like the isolated PKCα C2 domain, the isolated $cPLA_2\alpha$ C2 domain is fully functional as a targeting motif, and its mechanism of membrane specificity can be studied in the absence of the catalytic domain.

Previous studies have identified target lipids proposed to dominate membrane recognition during the Ca^{2+}-triggered membrane-docking reactions of C2 domains. For the PKCα C2 domain, the primary target lipids appear to be PS and PIP_2 (*12*, *23*, *27*), whereas for the $cPLA_2\alpha$ C2 domain, the primary target lipid is PC (*10*, *12*, *52*). However, no *in vitro* study has yet successfully reproduced C2 domain targeting under physiological conditions. During a typical cytoplasmic Ca^{2+} signal, the bulk Ca^{2+} concentration rises from approximately 0.1 μM up to a peak level of 0.5−0.9 μM, thus approaching but rarely exceeding 1 μM (*53*). In the cytoplasmic compartment, the effective concentration of lipids on the plasma membrane inner leaflet is approximately 400−800 μM, whereas the effective concentration of lipids on the cytoplasmic leaflet of the nuclear−Golgi−ER membrane system is much higher (*54*). Current models propose that C2 domain docking and membrane specificity are driven purely by interactions of the C2 domain with the structural and electrostatic features of lipid bilayers, including specific lipid headgroups, without contributions from protein−protein interactions (*10*, *12*, *25*, *27*). If this hypothesis is true, then it should be possible to find lipid mixtures that enable C2 domain docking to specific target membranes at micromolar Ca^{2+} concentrations. It is crucial to carry out such *in vitro* studies at physiological concentrations of Ca^{2+} because previous studies have demonstrated that super-physiological concentrations of Ca^{2+} can drive docking to membranes even when they are missing an important targeting element (*10*, *12*, *27*).

The present study compares the intracellular Ca^{2+}-activated targeting of the isolated PKCα- and $cPLA_2\alpha$-C2 domains in a macrophage model system. Subsequently, synthetic lipid mixtures are used *in vitro* to determine the lipid components and concentrations needed to drive membrane association at micromolar Ca^{2+} concentrations. Both the equilibrium and kinetic features of these interactions are investigated. The results further define the lipid bilayer features required for efficient Ca^{2+}-driven targeting of these two C2 domains to specific membrane surfaces under physiological conditions and further illuminate the molecular events that occur during these targeting reactions.

MATERIALS AND METHODS

Reagents. All lipids were synthetic unless otherwise indicated. 1-Palmitoyl-2-oleoyl-*sn*-glycero-3-phosphocholine (phosphatidylcholine, POPC, PC) and 1-palmitoyl-2-arachidonoyl-*sn*-glycero-3-phosphocholine (phosphatidylcholine, PAPC); 1-palmitoyl-2-oleoyl-*sn*-glycero-3-phosphoethanolamine (phosphatidylethanolamine, PE); phosphatidylinositol (PI) natural from bovine liver; 1-palmitoyl-2-oleoyl-*sn*-

[1] Abbreviations: $cPLA_2\alpha$, the α-isoform of cytosolic phospholipase A_2; PKCα, the α-isoform of protein kinase C; PC, phosphatidylcholine; PS, phosphatidylserine; PIP_2, phosphatidylinositol-4,5-bisphosphate; MATA, messenger-activated target affinity; TAMA, target-activated messenger-affinity; CFP, cyan fluorescent protein; RFP, red fluorescent protein; YFP, yellow fluorescent protein.

glycero-3-phosphoserine (phosphatidylserine, PS); sphingomyelin (SM) natural from brain; and dipalmitoyl-D-*myo*-phosphatidylinositol-4,5-bisphosphate (PI(4,5)P_2) natural from brain were all from Avanti Polar Lipids. Cholesterol (CH) was from Sigma. *N*-[5-(Dimethylamino)naphthalene-1-sulfonyl]-1,2-dihexadecanoyl-*sn*-glycero-3-phosphoethanolamine (dansyl-PE, dPE) was from Molecular Probes.

Fusion Protein Constructs. A plasmid encoding the murine cPLA$_2\alpha$ C2 domain fused to the C-terminus of mRFP1 (RFP-cPLA$_2\alpha$C2) was constructed by amplifying IMAGE clone BC003816 using primers that generated XhoI and XmaI sites on the polymerase chain reaction (PCR) product and ligating the digested product into complementary sites in pmRFP1-(C3), a plasmid constructed by substituting mRFP1 for EGFP in pEGFP(C3) (BD Biosciences Clontech). The resulting construct, RFP-cPLA$_2\alpha$C2, encodes residues 17 to 148 of the murine cPLA$_2\alpha$ protein and includes the entire C2 domain. The plasmid encoding the human PKCα C2 domain fused to YFP (YFP-PKCαC2) was previously described (*13*). For *in vitro* lipid-binding studies, the PKCαC2 and cPLA$_2\alpha$C2 domains were subcloned by PCR into the EagI/EcoR1 site of a glutathione *S*-transferase (GST)-fusion vector as previously described (*27*).

Cell Culture. RAW264.7 cells obtained from American Type Culture Collection (Manassas, VA) were plated on 35 mm glass-bottomed dishes (MatTek, Ashland, MA) at a density of 1×10^4 cells/cm^2 and cultured in DMEM containing 10% heat-inactivated FBS, 100 U/mL penicillin, 100 μg/mL streptomycin, 0.292 mg/mL glutamine, and 20 mM HEPES in 5% CO_2 at 37 °C. The cells were transfected with 1−2.5 μg each of the relevant plasmids using Lipofectamine 2000 (Invitrogen) in OptiMEM (Invitrogen), following the manufacturer's protocol.

Microscopy of Fluorescent Proteins. Cotransfected RAW264.7 cells were rinsed with and incubated in HBSS additionally buffered with 25 mM HEPES at pH 7.4 (HHBSS) containing 0.01% endotoxin-free BSA. Images were acquired using a Nikon inverted microscope equipped with a 60 × 1.4 N.A. oil immersion objective, a CFP/YFP/RFP dichroic mirror, corresponding single band excitation and emission filters (Chroma Technology), and a CoolSNAP ES camera (Photometrics, Tucson, AZ). Excitation light was provided by a mercury lamp. Cells were stimulated with 5 μM ionomycin between the acquisition of the first and second YFP/RFP image sets. Each image set began with 300 ms YFP and 300 ms RFP acquisitions, followed by a closed shutter period, yielding a total interval of 3 s between the starting points of subsequent image sets. Final images were produced using Adobe Photoshop (Adobe) and ImageJ (NIH, http://rsb.info.nih.gov/ij/).

Expression and Purification of Isolated C2 Domains. The C2 domains of PKCα and cPLA$_2\alpha$ were expressed as glutathione *S*-transferase (GST)-fusion proteins and isolated on a glutathione affinity column prior to cleavage with thrombin and elution of the free C2 domain. The free cPLA$_2$-C2 domain was further purified by Ca^{2+}-dependent binding to PC-phenyl sepharose resin, followed by elution with ethylenediaminetetraacetic acid (EDTA) as described (*45*). The mass of the PKCα-C2 and cPLA$_2\alpha$-C2 domains were confirmed by matrix-assisted laser desorption/ionization time-of-flight mass spectroscopy (MALDI-TOF). Protein purity was determined by SDS−PAGE (*55*), and protein concentration was determined by both absorbance at 280 nm using the calculated extinction coefficient and by the tyrosinate difference spectral method (*56*).

Preparation of Lipid Mixtures and Phospholipid Vesicles. Lipids were dissolved in chloroform/methanol/water (1/2/0.8) to give the desired lipid ratios, dried under vacuum at 45 °C until all solvents were removed, and then hydrated with buffer A (25 mM *N*-(2-hydroxyethyl)piperazine-*N*′-2-ethanesulfonic acid (HEPES) at pH 7.4 with KOH, 140 mM KCl, 15 mM NaCl, and 1 mM $MgCl_2$) by rapid vortexing. Small unilamellar phospholipid vesicles were generated by sonication of the hydrated lipids to clarity with a Misonix XL2020 probe sonicator. The vesicle stock solutions used in the equilibrium calcium titrations and kinetic experiments were prepared with a total lipid concentration of 3 mM with the following mole percentages for simple membranes: PE/PC/PS/dPE (65/10/20/5) and PE/PC/PS/dPE (40/50/5/5); for physiological plasma membrane variations: PM [6% PIP_2], CH/PE/PS/PC/PIP_2/dPE/PI/SM (25/23.5/21/10.5/6/5/4.5/4.5); PM [2% PIP_2], PE/CH/PS/PC/dPE/PI/SM/PIP_2 (27.5/25/21/10.5/5/4.5/4.5/2); PM [6% PIP_2] (−) PS, PE/CH/PC/PIP_2/dPE/PI/SM (44.5/25/10.5/6/5/4.5/4.5); PM [2% PIP_2] (−) PS, PE/CH/PC/dPE/PI/SM/PIP_2 (48.5/25/10.5/5/4.5/4.5/2); PM [0% PIP_2, 5%CH], PE/PS/PC/CH/dPE/PI/SM (49.5/21/10.5/5/5/4.5/4.5); PM [0% PIP_2], PE/CH/PS/PC/dPE/PI/SM (29.5/25/21/10.5/5/4.5/4.5); PM [0% PIP_2, 38.5% PC], PC/CH/PS/dPE/PI/SM/PE (38.5/25/21/5/4.5/4.5/1.5); and PM [0% PIP_2] (−) PS, PE/CH/PC/dPE/PI/SM (50.5/25/10.5/5/4.5/4.5); and for physiological internal membrane variations: IM, PC/PE/CH/dPE/PS/PI/SM (49.5/27/5/5/4.5/4.5/4.5); IM [12%PS], PC/PS/PE/CH/ dPE/PI/SM (49.5/21/10.5/5/5/4.5/4.5); IM [25%CH], PC/CH/PE/dPE/PS/PI/SM (49.5/25/7/5/4.5/4.5/4.5); IM [13.5%PC], PE/PC/CH/dPE/PS/PI/SM (63/13.5/5/5/4.5/4.5/4.5). Table 1 summarizes these lipid mixtures. Additional vesicle stock solutions for use in the equilibrium calcium titrations that required final total lipid concentrations greater than 200 μM were prepared at a total lipid concentration of 30 mM with the following mole percentages: PE/CH/PS/PC/dPE/PI/SM/PIP_2 (28.5/25/21/10.5/5/4.5/4.5/1) and PC/PE/CH/dPE/PS/PI/SM (49/27/5/5/4.5/4.5/4.5). Following sonication, the insoluble material was removed from all lipid mixtures by centrifugation at 17,970*g* for 5 min.

Steady-State Fluorescence Spectoscopy. Steady-state fluorescence experiments were carried out on a Photon Technology International QM-2000-6SE fluorescence spectrometer at 25 °C in buffer A. The excitation and emission slit widths were 1 and 8 nm, respectively, for all measurements. All buffers were made with Chelex-treated Ca^{2+}-free water. Protein and lipid solutions were incubated with Chelex resin to remove residual Ca^{2+} before use. Quartz cuvettes and stir bars were decalcified by soaking in 100 mM EDTA and extensive rinsing with Ca^{2+}-free water prior to use (*10*, *23*, *45*).

Measurement of Equilibrium Ca^{2+}-Dependent Protein-to-Membrane FRET. The quantitation of the Ca^{2+}-dependent increase in protein-to-membrane FRET for C2 domain binding to membranes was carried out according to previously developed methods (*10*, *23*, *45*). Briefly, Ca^{2+}-free C2 domain (0.75 μM) and Ca^{2+}-free sonicated lipids (200 μM total = 100 μM accessible, except where indicated otherwise) in buffer A were mixed with a small volume of a concentrated Ca^{2+} stock solution in buffer A, and the protein-to-

Table 1: Mole Percentages of Synthetic Membrane Lipid Components: Plasma Membrane Variants and Internal Membrane Variants

Plasma Membrane Variants								
lipid	PM [6%PIP_2]	PM [2%PIP_2]	PM [6%PIP_2] (−)PS	PM [2%PIP_2] (−)PS	PM [0%PIP_2] [5%CH]	PM [0%PIP_2]	PM [0%PIP_2] [38.5%PC]	PM [0%PIP_2] (−)PS
PE	23.5	27.5	44.5	48.5	49.5	29.5	1.5	50.5
PC	10.5	10.5	10.5	10.5	10.5	10.5	38.5	10.5
PS	21	21	0	0	21	21	21	0
PI	4.5	4.5	4.5	4.5	4.5	4.5	4.5	4.5
SM	4.5	4.5	4.5	4.5	4.5	4.5	4.5	4.5
CH	25	25	25	25	5	25	25	25
PIP_2	6	2	6	2	0	0	0	0
dPE	5	5	5	5	5	5	5	5

Internal Membrane Variants				
lipid	IM	IM [21%PS]	IM [25%CH]	IM [13.5%PC]
PE	27	10.5	7	63
PC	49.5	49.5	49.5	13.5
PS	4.5	21	4.5	4.5
PI	4.5	4.5	4.5	4.5
SM	4.5	4.5	4.5	4.5
CH	5	5	25	5
dPE	5	5	5	5

membrane FRET was quantitated from dPE emission (excitation and emission wavelengths were $\lambda_{ex} = 284$ nm and $\lambda_{em} = 522$ nm, respectively). In a separate sample, identical Ca^{2+} was added to a Ca^{2+}-free lipid solution in buffer A lacking protein to control for any changes in background emission arising from light scattering associated with Ca^{2+}-mediated liposome aggregation and photobleaching of the dPE. Following the correction for dilution and subtraction of the background emission, the Ca^{2+} dependence of the fluorescence increase (ΔF) was plotted as a function of free Ca^{2+} ($[Ca^{2+}]$), and the best fit was obtained using the following Hill equation (eq 1):

$$\Delta F = \Delta F_{max}\left(\frac{[Ca^{2+}]^H}{[Ca^{2+}]_{1/2}{}^H + [Ca^{2+}]^H}\right) \quad (1)$$

where ΔF_{max} represents the calculated maximal fluorescence change (normalized to unity, except where noted otherwise, to simplify graphical presentations), H represents the Hill coefficient, and $[Ca^{2+}]_{1/2}$ represents the free Ca^{2+} concentration that induces a half-maximal fluorescence change. In most cases, the free Ca^{2+} concentration was estimated to be the same as the concentration of Ca^{2+} added to the decalcified reaction solution over the course of the titration. This approximation yielded accurate $[Ca^{2+}]_{1/2}$ values when $[Ca^{2+}]_{1/2}$ values sufficiently exceeded the concentration of the C2 domain present in the decalcified starting reaction (0.75 μM). For $[Ca^{2+}]_{1/2}$ values below 4 μM, the free Ca^{2+} concentration was calculated by correcting the total Ca^{2+} concentration for Ca^{2+} bound to the C2 domain and for trace background amounts of Ca^{2+} present after decalcification.

Stopped-Flow FRET Measurements of Association and Dissociation Kinetics. All kinetic experiments were done on an Applied Photophysics SX.17 stopped-flow fluorescence instrument at 25 °C in buffer A as previously described (*10*, *23*, *45*) with the following modifications. The deadtime of the instrument was 0.9 ± 0.1 ms; thus, all data points prior to 1 ms were eliminated prior to quantitative analysis. To measure the protein-to-membrane FRET in this instrument, the excitation wavelength and slit-width settings on the excitation monochromator were 284 and 6 nm, respectively, whereas a 475 nm long-pass filter was used to select the detected wavelengths of emitted light.

To determine the observed rate constant for membrane association (k_{obs}), C2 domains (1 μM, all concentrations prior to mixing) and Ca^{2+} (5, 50, or 1000 μM) in buffer A were mixed by stopped-flow with vesicles (400 μM total lipid) in the same buffer and Ca^{2+} concentration. The resulting time course yielded an increasing protein-to-membrane FRET with time and was subjected to nonlinear least-squares best-fit analysis using the following single-exponential function (eq 2).

$$F = \Delta F_{max}\,(1 - e^{-k_{obs}\cdot t}) + C \quad (2)$$

To simplify graphical presentations, the best-fit offset C was subtracted from all data points, and the best-fit ΔF_{max} value was normalized to unity.

To determine the rate constant for the dissociation (k_{off}) of C2 domains from the membranes, the experiment began with the preformed ternary complex of the C2 domain (1 μM), vesicles (400 μM total lipid), and Ca^{2+} (5, 10, or 1000 μM) in buffer A. At time zero, the ternary complex was rapidly mixed with an equal volume of EDTA (20 mM) in the same buffer. The resulting approach to equilibrium was monitored as a decrease in the protein-to-membrane FRET as the C2 domain dissociated from the membrane. The time course was subjected to nonlinear least-squares best-fit analysis using a single- or double-exponential function eq 3 or 4, respectively.

$$F = \Delta F_{max}\,(e^{-k_{off}\cdot t}) + C \quad (3)$$

$$F = \Delta F_{max_1}\,(e^{-k_{off1}\cdot t}) + \Delta F_{max_2}\,(e^{-k_{off2}\cdot t}) + C \quad (4)$$

To simplify graphical presentations, the best-fit offset C was subtracted from all data points, and the best-fit ΔF_{max} (or,

for the latter equation, $\Delta F_{max_1} + \Delta F_{max_2}$) value was normalized to unity.

RESULTS

Strategy. The present study investigates the mechanism of Ca^{2+}-activated targeting of C2 domains to specific intracellular membranes, using the C2 domains of the important signaling enzymes PKCα and $cPLA_2α$ as representative examples. Previous studies carried out in various cell types have found that cytoplasmic Ca^{2+} signals drive the PKCα C2 domain primarily to the plasma membrane, whereas the $cPLA_2α$ C2 domain primarily targets to internal membranes (*12*, *13*, *27*, *46*, *57*). Previous *in vitro* studies have established important elements of this specificity: PKCα C2 prefers membranes containing phosphatidylserine (PS) (*12*, *23*) and phosphatidylinositol-4,5-bisphosphate (PIP_2) (*27*), whereas $cPLA_2α$ C2 prefers membranes rich in phosphatidylcholine (PC) (*10*, *12*, *52*). But previous *in vitro* studies have not yet rigorously explained the highly efficient and specific membrane docking of these C2 domains at the bulk concentration of Ca^{2+} achieved in the cytoplasm during the peak of a typical Ca^{2+} signaling event (approximately 500 to 900 nM, hereafter referred to as 1 μM) (*53*).

To directly compare the membrane-targeting specificities of the PKCα and $cPLA_2α$ C2 domains, the present study begins by coexpressing the two domains in RAW264.7 cells, a macrophage cell line. Subsequent *in vitro* studies are designed to analyze the mechanism of specific membrane targeting using synthetic membranes composed of carefully controlled lipid mixtures. To determine the lipid mixtures and concentrations needed to achieve physiological membrane targeting, the present study employs model membranes composed of both simple and complex lipid mixtures, the latter designed to closely approximate the cytosolic leaflets of plasma and intracellular membranes. A protein-to-membrane FRET assay is used to elucidate the equilibrium and kinetic parameters for C2 domain docking to these model membranes *in vitro*. The approach provides new insights into the mechanisms of target-membrane recognition by the PKCα and $cPLA_2α$ C2 domains and into the molecular events that occur during Ca^{2+}-activated membrane docking.

Ca^{2+}-Dependent Membrane Targeting of PKCα-C2 and $cPLA_2$-C2 Domains in Living Cells. The PKCα and $cPLA_2α$ C2 domains were fused to yellow fluorescent protein (YFP) and red fluorescent protein (RFP), respectively. The resulting fusion proteins were simultaneously introduced into the mouse macrophage cell line, RAW264.7, and the fluorescent cells were treated with the Ca^{2+} ionophore ionomycin to elicit a homogeneous cytoplasmic Ca^{2+} increase of magnitude approximating the micromolar peak of a physiological Ca^{2+} signal ((*58*) and Evans, unpublished results), as illustrated in Figure 1. In untreated cells, both fusion proteins exhibited a uniform distribution in the cytoplasm and nucleoplasm (Figure 1A and C). Within seconds of the cytoplasmic Ca^{2+} increase, YFP-PKCαC2 translocated to the plasma membrane and RFP-$cPLA_2α$C2 to the internal membranes (Figure 1B and D). Notably, the merged image (Figure 1E, PKCαC2 in green and $cPLA_2α$C2 in red) highlights the mutually exclusive targeting of the two C2 domains, consistent with previous findings that the PKCα C2 domain exclusively targets the plasma membrane, whereas the $cPLA_2α$ C2 domain exclusively targets the internal membranes (*12*, *13*, *27*, *46*, *57*).

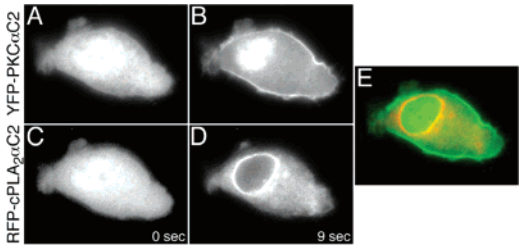

FIGURE 1: Coexpression and Ca^{2+}-activated targeting of the PKCα and $cPLA_2$-C2 domains in a macrophage-derived cell line. Shown are (A and B) yellow and (C and D) red fluorescent protein fusions of the PKCα- and $cPLA_2$-C2 domains, respectively, coexpressed in the same RAW264.7 cell. The images at time zero (A and C) illustrate the distributions of the two fluorescent proteins throughout the cytoplasmic and nuclear compartments just prior to the addition of ionomycin, which triggered a global Ca^{2+} signal. Within 9 s after this addition, (B) the PKCα C2 domain was recruited from the cytoplasm to the plasma membrane, and (D) the $cPLA_2$ C2 domain was recruited from the cytoplasm and nuclear compartments to the nuclear, Golgi, and ER membranes. The overlay of the latter two images (E) reveals the exclusive, non-overlapping targeting of these two C2 domains to plasma and internal membranes, respectively. For simplicity, the images shown are mid-plane slices through the cell. Such mid-plane images do not display the punctate pattern of fluorescence observed for the PKCα-C2 domain recruitment to the apical and basal surfaces of the plasma membrane (*27*). Moreover, these transient transfections do not exhibit the cell polarization observed for stably transfected RAW cells under similar conditions (Evans, J. H., and Falke, J. J., unpublished work).

Similar targeting specificities have been observed for these two C2 domains in other cell types (*12*, *13*, *27*, *46*, *57*). The most variability is observed for the $cPLA_2α$ C2 domain, which in RAW cells primarily targets to the nuclear membrane, whereas a small but detectable fraction of the C2 domain population targets to the Golgi and endoplasmic reticulum (ER) membranes. The same type of targeting pattern, primarily localized to the nuclear membrane, has been previously observed in primary leukocytes and in HEK293 cells, both of which possess a relatively small density of Golgi membranes (*12*, *46*). By contrast, in CHO and MDCK cells, both of which possess extensive Golgi systems, the $cPLA_2α$ C2 domain primarily targets to Golgi rather than to other internal membranes (*13*, *27*, *59*). Thus, the distribution of the $cPLA_2α$ C2 domain between the nuclear, Golgi, and ER membranes is closely tied to the relative densities of these membrane systems in the cell interior. In cell types with poorly developed Golgi systems, most of the targeting is to the nuclear membrane, whereas in cell types with extensive Golgi systems, the majority of targeting is to the Golgi membrane.

PKCα-C2 and $cPLA_2$-C2 Domain Expression and Purification. Recombinant PKCα-C2 and $cPLA_2α$-C2 domains were cloned, expressed, and purified (see Materials and Methods) for use in model membrane-binding studies designed to investigate the mechanisms of specific membrane targeting at physiological Ca^{2+} concentrations. The purity of the resulting domains was determined by SDS−PAGE and was found to exceed 90%. The masses of PKCα-C2 and $cPLA_2α$-C2 were found to be 16,288 and 16,267 Da, respectively, by MALDI-TOF mass spectroscopy. Both experimental masses are within the error of the predicted masses (16,283 for PKCα-C2 and 16,267 for $cPLA_2α$-C2).

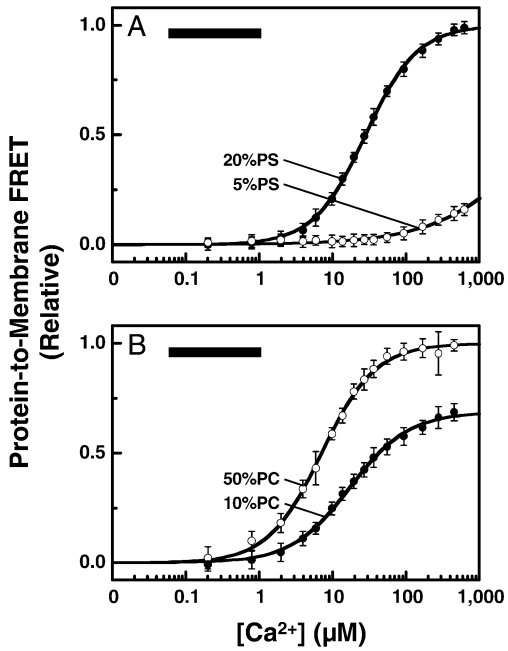

FIGURE 2: Equilibrium binding of the PKCα- and cPLA$_2$α-C2 domains to simple lipid mixtures of phosphatidylcholine (PC), phosphatidylserine (PS), and phosphatidylethanolamine (PE). Shown are Ca^{2+} titration curves for the Ca^{2+}-triggered docking of (A) PKCα-C2 and (B) cPLA$_2$α-C2 to sonicated unilamellar vesicles composed of simple lipid mixtures crudely resembling the inner leaflet of the plasma membrane (PE/PC/PS/dPE, 65/10/20/5 mol %) or internal membranes (PE/PC/PS/dPE, 40/50/5/5 mol %). The PKCα-C2 domain was observed to prefer the simple plasma membrane mimic containing 20 mol % PS over the internal membrane mimic containing 5 mol % PS, whereas the cPLA$_2$α-C2 domain showed a weaker preference for the simple internal membrane mimic containing 50 mol % PC over the simple plasma membrane mimic containing 10 mol % PC. However, both of the C2 domain−membrane combinations failed to yield substantial membrane docking in the physiological range of Ca^{2+} concentrations observed in the bulk cytoplasm (black bar). Membrane docking was quantitated by measuring protein-to-membrane FRET between native Trp donors in the protein and a dansylated phosphatidylethanolamine (dPE) acceptor present at low levels in the membrane. The solid curves represent the best fits with the Hill equation (eq 1). Within each box, the upper curve is normalized so that it asymptotically approaches unity, whereas the other curves are plotted on the same relative fluorescence scale, emphasizing their different equilibrium levels of protein-to-membrane FRET at saturating $[Ca^{2+}]$.

Equilibrium Ca^{2+} Dependence of PKCα-C2 and cPLA$_2$-C2 Domain Targeting to Simple Model Membranes. The affinities of PKCα-C2 and cPLA$_2$α-C2 for membranes have been shown to be strongly dependent on membrane PS and PC content, respectively, under conditions of super-physiological Ca^{2+} concentrations (100−1000 μM) (*10*, *12*, *23*, *52*). To examine whether simple lipid mixtures containing PS and PC can reproduce *in vitro* the micromolar Ca^{2+} sensitivity and orthogonal target membrane specificities observed for these C2 domains, the binding of C2 domains to synthetic sonicated, small unilamellar vesicles (SUVs) composed of simple PS and PC mixtures was examined. Protein-to-membrane FRET was employed to measure membrane docking as Ca^{2+} was titrated into a solution containing a given domain, a given type of SUV, and a physiological buffer ((*45*), see Materials and Methods).

For the PKCα-C2 domain, the Ca^{2+} titration profile in Figure 2A yielded a nonlinear least-squares best-fit $[Ca^{2+}]_{1/2}$ of 28 ± 2 μM for C2 domain docking to simple membranes with a PS content of 20 mol %, approximating the PS content of its target membrane, the inner leaflet of the plasma membrane (PE/PC/PS/dPE, 65/10/20/5 mol %) (*12*, *60*, *61*). By contrast, the $[Ca^{2+}]_{1/2}$ exceeded 1000 μM for C2 domain docking to membranes containing 5 mol % PS, corresponding to the PS content of internal membranes (PE/PC/PS/dPE, 40/50/5/5 mol %) (*12*, *60*, *61*).

For the cPLA$_2$α-C2 domain, the Ca^{2+} titration in Figure 2B yielded a $[Ca^{2+}]_{1/2}$ of 7 ± 1 μM for C2 domain docking to membranes containing 50 mol % PC, resembling the PC content of its target internal membranes (PE/PC/PS/dPE, 40/50/5/5 mol %) (*12*, *60*, *61*). A $[Ca^{2+}]_{1/2}$ of 17 ± 2 μM was observed for C2 domain docking to membranes containing 10 mol % PC, as in the plasma membrane inner leaflet (PE/PC/PS/dPE, 65/10/20/5 mol %) (*12*, *60*, *61*).

These Ca^{2+} titrations for simple lipid mixtures confirm the previously noted PS and PC preferences of the PKCα-C2 and cPLA$_2$α-C2 domains, respectively (*10*, *12*, *23*, *52*). Such preferences make significant contributions to the intracellular targeting of the two domains because the highest PS and PC lipid mole percentages are found in the plasma and internal membranes, respectively (*12*, *60*, *61*). However, under the present experimental conditions, the Ca^{2+} titrations for simple PS/PC mixtures yield nonphysiological $[Ca^{2+}]_{1/2}$ values that are 28-fold and 7-fold too large, respectively, to explain the efficient docking of the PKCα- and cPLA$_2$α-C2 domains to their target membranes during micromolar cytoplasmic Ca^{2+} signaling events. Recently, we observed that the addition of PIP$_2$ to simple PS/PC membranes yielded a significantly lower $[Ca^{2+}]_{1/2}$ value; however, this value remained at least 3-fold too large to explain efficient docking during a micromolar cytoplasmic Ca^{2+} signal. In an effort to identify the protein−membrane interactions that bring the Ca^{2+} affinities of the PKCα- and cPLA$_2$α-C2 domains into the physiological range, further experiments were conducted with synthetic membranes that more closely approximate the complexity of physiological membranes.

Complex, Physiological Model Membranes Designed to Mimic Target Intracellular Membranes. Physiological model membrane SUVs were generated with lipid compositions designed to mimic the cytosolic leaflet of either the plasma membrane or the internal cell membranes. These model membranes, detailed in Table 1, contained the predominant lipids of mammalian membranes exposed to the cytoplasm, including phosphatidylethanolamine (PE), phosphatidylcholine (PC), phosphatidylserine (PS), phosphatidylinositol (PI), sphingomyelin (SM), cholesterol (CH), and phosphatidylinositol-4,5-bisphosphate (PIP$_2$) as well as a small density of the FRET acceptor dansyl-phosphatidylethanolamine (dPE, 5 mol %). The plasma membrane mimic (PM) reflects the relatively high content of PS, cholesterol, and PIP$_2$ and the low content of PC, found in the plasma membrane inner leaflet ((*12*, *60*, *61*), Table 1). Two versions of this PM mixture were utilized containing 21 mol % PS and either 2 mol % PIP$_2$, corresponding to the bulk PIP$_2$ concentration of the plasma membrane inner leaflet, or 6 mol % PIP$_2$, representing the putative local PIP$_2$ concentration in lipid rafts (*62*−*65*). The internal membrane mimic (IM) reflects the high content of PC, approaching 50 mol %, as well as the low content of PS, cholesterol, and PIP$_2$ found in internal cell membranes, such as nuclear, Golgi, and ER membranes

(*12*, *60*, *61*). Additional lipid mixtures based on variations of the PM and IM mixtures were also created to examine the roles of specific lipid components in membrane recognition by C2 domains. These variations lowered the mole percentage of PC, PS, CH, or PIP_2 while correspondingly increasing the mole percent of PE, thereby maintaining constant densities of all other components (Table 1). Both previous work and the results from this study indicate that the PKCα-C2 and $cPLA_2$α-C2 domains are relatively insensitive to membrane PE content (*10*, *12*, *23*, *52*), making PE the best choice for a replacement component. Preliminary studies comparing the binding of C2 domains to SUVs versus large unilamellar vesicles (LUVs) of the same lipid composition revealed no detectable differences (data not shown), suggesting that the greater membrane curvature of SUVs does not significantly alter protein−membrane interactions in this system.

*Ca^{2+} Dependence of PKC*α-C2 *Domain Docking to Physiological Model Membranes*. The protein-to-membrane FRET assay was used to measure membrane docking as Ca^{2+} was titrated into the system containing the PKCα-C2 domain and a given type of physiological model membrane SUVs, thereby revealing the effects of different lipid mixtures on the Ca^{2+} dependence of membrane docking. Figure 3A shows the resulting Ca^{2+} titration curves, and Table 2 summarizes the corresponding $[Ca^{2+}]_{1/2}$ values, determined by nonlinear least-squares best-fit using the Hill equation. Each Hill analysis utilized the actual free Ca^{2+} concentration calculated for the relevant titration by correcting for minimal background Ca^{2+} contamination (0.1 μM) and for Ca^{2+} bound to the C2 domain (see Materials and Methods).

The results of Figure 3A and Table 2 indicate that PM mixtures containing physiological levels of both PS and PIP_2 yield high Ca^{2+} affinities that are adequate to explain the observed recruitment of the PKCα-C2 domain to the inner leaflet of the plasma membrane during cytoplasmic Ca^{2+} signals. The PM mixture containing 2 mol % PIP_2, designated PM[2%PIP_2], yielded a $[Ca^{2+}]_{1/2}$ value of 1.6 ± 0.1 μM. Similarly, the PM mixture containing 6 mol % PIP_2, designated PM[6%PIP_2], yielded a $[Ca^{2+}]_{1/2}$ value of 0.7 ± 0.1 μM (Figure 3A, Table 2). By contrast, the IM mixture yielded much weaker Ca^{2+}-triggered membrane binding such that the measured $[Ca^{2+}]_{1/2}$ greatly exceeded 300 μM (Figure 3A, Table 2). These findings confirm that physiological lipid mixtures resembling the cytosolic leaflet of the plasma membrane but not that of inner membranes enable efficient recruitment of the PKCα-C2 domain at micromolar levels of Ca^{2+}.

The results further indicate that efficient docking of the PKCα-C2 domain to model physiological membranes at micromolar Ca^{2+} levels requires both PS and PIP_2 but is significantly less sensitive to PC and cholesterol. Thus, when the PS was removed from the PM mixture, yielding either the PM[2%PIP_2](−)PS or the PM[6%PIP_2](−)PS mixture, $[Ca^{2+}]_{1/2}$ increased 7-fold or 5-fold, respectively (Figure 3A, Table 2). Similarly, when PIP_2 was removed from the PM mixture, yielding the PM(−)PIP_2 mixture, $[Ca^{2+}]_{1/2}$ increased 20-fold or 50-fold, relative to the corresponding PM mixtures containing 2 or 6 mol % PIP_2, respectively (Figure 3A, Table 2). Finally, when both PS and PIP_2 were removed to yield the PM(−)PIP_2(−)PS mixture, $[Ca^{2+}]_{1/2}$ increased to a value greatly exceeding 300 μM, similar to that observed for IM membranes (Figure 3A, Table 2). By contrast, the $[Ca^{2+}]_{1/2}$ value was found to be relatively independent of the PC or cholesterol content as long as lipid mixtures containing similar levels of PS and PIP_2 were compared (Figure 3A, Table 2). Together, these results indicate that the exquisite plasma membrane targeting specificity of the PKCα-C2 domain triggered by a micromolar cytoplasmic Ca^{2+} signal is highly dependent on only the PS and PIP_2 contents of the target membrane.

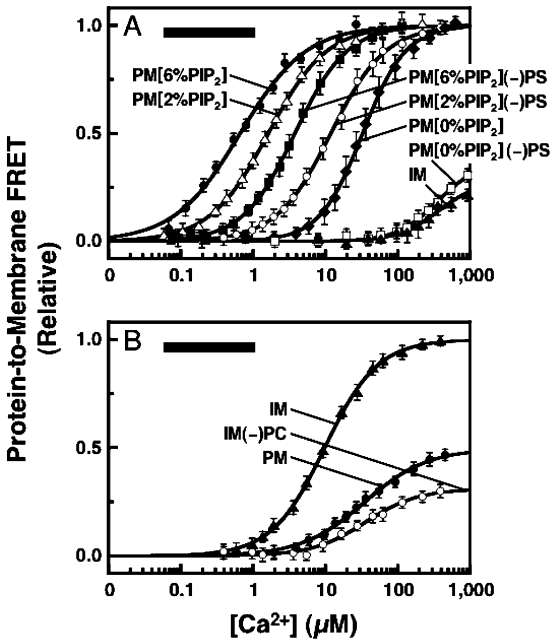

FIGURE 3: Equilibrium binding of the PKCα- and $cPLA_2$α-C2 domains to physiological lipid mixtures. Shown are Ca^{2+} titration curves for the Ca^{2+}-triggered docking of (A) PKCα-C2 and (B) $cPLA_2$α-C2 to sonicated unilamellar vesicles composed of complex, physiological lipid mixtures containing phosphatidylethanolamine (PE), cholesterol (CH), phosphatidylserine (PS), phosphatidylcholine (PC), phosphatidylinositol (PI), sphingomyelin (SM), and phosphatidylinositol-4,5-bisphosphate (PIP_2). The membranes labeled PM[2% PIP_2] and PM[6% PIP_2] mimicked the plasma membrane inner leaflet (PE/CH/PS/PC/dPE/PI/SM/PIP_2, mole percentages (27.5 or 23.5)/25/21/10.5/5/4.5/4.5/(2 or 6), whereas the membrane labeled IM mimicked the internal membranes (PC/PE/CH/dPE/PS/PI/SM, mole percentages 49.5/27/5/5/4.5/4.5/4.5). Other membranes were created by modifying these two basic mixtures in order to test the importance of individual components, yielding the compositions summarized in Table 1. (A) The PKCα-C2 domain exhibited high specificity for plasma membrane mimics PM[2% PIP_2] and PM[6% PIP_2] and was effectively recruited by these membranes at physiological Ca^{2+} concentrations (black bar). In contrast, the internal membrane mimic IM and membranes lacking PS, PIP_2, or both of these target lipids failed to recruit this C2 domain at physiological Ca^{2+} concentrations. (B) The $cPLA_2$α-C2 domain exhibited weaker specificity for the internal membrane mimic (IM) relative to that for the plasma membrane mimic (PM-[6% PIP_2]) and was poorly recruited by membranes at physiological Ca^{2+} concentrations (black bar). Removal of the target lipid PC (IM (−) PC) significantly reduced the affinity of this C2 domain for the membrane. Protein docking to the membrane was quantitated by protein-to-membrane FRET as described in the legend for Figure 2. The solid curves represent the best fits with the Hill equation (eq 1), yielding the $[Ca^{2+}]_{1/2}$ values and Hill coefficients summarized in Table 2. Within each box, the upper curve is normalized so that it asymptotically approaches unity, whereas other curves are plotted on the same relative fluorescence scale to highlight different equilibrium levels of protein-to-membrane FRET at saturating $[Ca^{2+}]$.

Table 2: Equilibrium Parameters for C2 Domain Docking to Synthetic Membranes

C2 domain	lipid mixture	$[Ca^{2+}]_{1/2}$ (μM)	Hill coefficient
PKCα-C2	PM[6%PIP_2]	0.7 ± 0.1	1.0 ± 0.1
	PM[2%PIP_2]	1.6 ± 0.1	1.0 ± 0.1
	PM[6%PIP_2](−)PS	3.8 ± 0.1	1.0 ± 0.5
	PM[2%PIP_2] (−)PS	12 ± 3	1.2 ± 0.2
	PM[0%PIP_2, 5%CH]	21 ± 4	1.2 ± 0.1
	PM[0%PIP_2]	33 ± 7	1.5 ± 0.1
	PM[0%PIP_2, 38.5%PC]	34 ± 3	1.7 ± 0.2
	PM[0%PIP_2](−)PS	350 ± 50	1.5 ± 0.1
	IM	360 ± 80	1.5 ± 0.5
$cPLA_2$α-C2	IM	10 ± 2	1.2 ± 0.1
	IM[21%PS]	9 ± 2	1.2 ± 0.1
	IM[25%CH]	11 ± 2	1.3 ± 0.2
	IM[13.5%PC]	36 ± 4	1.3 ± 0.1
	PM[6%PIP_2]	36 ± 3	1.2 ± 0.1
	PM[2%PIP_2]	31 ± 3	1.1 ± 0.1
	PM[0%PIP_2]	29 ± 4	1.2 ± 0.1

Table 3: $cPLA_2$α-C2 Docking to Synthetic Membranes Containing Potential Target Lipids[a]

lipid mixture	$[Ca^{2+}]_{1/2}$ (μM)	Hill coefficient
IM[100%POPC]	10 ± 2	1.3 ± 0.1
IM[50%POPC, 50%PAPC]	10 ± 2	1.2 ± 0.1
IM[100%PAPC]	7 ± 2	1.4 ± 0.2
IM[6%$PI(4)P_1$]	7 ± 1	1.2 ± 0.2
IM[10%Cer−1-P]	18 ± 1	1.0 ± 0.1

[a] Sonicated unilamellar vesicles were prepared as described in Materials and Methods from the following lipid mixtures: IM[100%POPC], POPC/PE/CH/dPE/PS/PI/SM (49.5/27/5/5/4.5/4.5/4.5); IM[50%POPC, 50%PAPC], PE/POPC/PAPC/CH/dPE/PS/PI/SM (27/24.75/24.75/5/5/4.5/4.5/4.5); IM[100%PAPC],PAPC/PE/CH/dPE/PS/PI/SM (49.5/27/5/5/4.5/4.5/4.5); IM[6% $PI(4)P_1$], POPC/PE/$PI(4)P_1$/CH/dPE/PS/PI/SM (49.5/21/6/5/5/4.5/4.5/4.5); IM[10%Cer-1-P], POPC/PE/Cer-1-P/CH/dPE/PS/PI/SM (49.5/17/10/5/5/4.5/4.5/4.5).

The presence of PIP_2 in the membrane was found to have a significant effect on the Hill coefficient for the Ca^{2+}-triggered docking of the PKCα C2 domain to membranes. Membranes lacking PIP_2 exhibited Hill coefficients ranging from 1.2 to 1.7 (Table 2), overlapping the value previously measured for Ca^{2+} titrations of PKCα-C2 domain docking to simple membranes lacking PIP_2 ($H = 1.3 \pm 0.1$, (*23*)). When PIP_2 was added, the Hill coefficient decreased slightly but significantly in most cases to values ranging from 1.0 to 1.2 (Table 2). The PKCα C2 domain possesses two Ca^{2+} binding sites, and the Hill coefficient for Ca^{2+}-triggered membrane docking reports positive cooperativity between these sites during the binding of two Ca^{2+} ions. The lower Hill coefficients observed for PIP_2-containing membranes suggest that PIP_2 facilitates the docking of the C2 domain containing only one bound Ca^{2+} ion, which would in principle exhibit a Hill coefficient of 1.0. This observation has important implications for the mechanism of membrane specificity and docking as further discussed below (see Discussion).

Ca^{2+} Dependence of $cPLA_2$-C2 Domain Docking to Physiological Model Membranes. For the $cPLA_2$α-C2 domain, Ca^{2+} titrations were also carried out using FRET to monitor C2 domain docking to physiological model membrane SUVs (Figure 3B). The resulting $[Ca^{2+}]_{1/2}$ values are summarized in Table 2. As previously observed, PC is the primary lipid determinant of $cPLA_2$α-C2 membrane docking specificity. Thus, the IM membrane mimic containing 50 mol % PC yielded a $[Ca^{2+}]_{1/2}$ value of 10 ± 2 μM such that membrane docking occurred at a 3-fold lower Ca^{2+} concentration than that for any of the PM mixtures containing 6, 2, or 0 mol % PIP_2 ($[Ca^{2+}]_{1/2} = 36 \pm 3$, 31 ± 3, or 29 ± 4 μM, respectively). The PC dependence of this specificity was investigated further using a series of IM mixtures with a low PC content, a high PS content, or a high CH content. A reduction in the PC content of the IM mixture to 13.5 mol % PC resulted in an increase in $[Ca^{2+}]_{1/2}$ of greater than 3-fold to 36 ± 3 μM, similar to the $[Ca^{2+}]_{1/2}$ value measured for the PM mixtures. By contrast, increases in the PS (to 21 mol %) or CH (to 25 mol %) content of the IM mixture, yielding levels of these lipids similar to those found in the plasma membrane, had little effect on Ca^{2+} sensitivity ($[Ca^{2+}]_{1/2} = 9 \pm 2$ and $[Ca^{2+}]_{1/2} = 11 \pm 2$ μM). For this C2 domain, the presence of PIP_2 in the membrane had no detectable effect on either the $[Ca^{2+}]_{1/2}$ value or the Hill coefficient, in contrast to the PKCα C2 domain where PIP_2 decreased both of these parameters (Table 2). This pattern is consistent with previous observations that unlike the PKCα C2 domain, the $cPLA_2$α-C2 domain possesses no PIP_2 binding site (*27*).

The present findings confirm that in the context of physiological lipid mixtures, membrane PC content has a role in defining $cPLA_2$α-C2 domain-targeting specificity. However, none of the membrane mimics, including the IM mixture, yielded $[Ca^{2+}]_{1/2}$ values within the micromolar range of Ca^{2+} concentrations found in cytoplasmic signals. It follows that the conditions of these *in vitro* experiments did not yet match those experienced by the $cPLA_2$α-C2 domain during intracellular targeting. One possible explanation was that the IM mixture might be missing an important lipid component. Three additional lipid components of internal membranes were tested as potential target lipids: ceramide-1-phosphate, $PI(4)P_1$, and arachidonate-containing PC. As summarized in Table 3, each of these additional lipids yielded less than a 2-fold effect on the $[Ca^{2+}]_{1/2}$ value, providing strong evidence that these lipids are not specific targets of the $cPLA_2$α-C2 domain. Thus, the evidence to date suggests that the only significant target lipid of this C2 domain is the PC headgroup, although an additional target cannot be ruled out. Another possible explanation for the micromolar values of $[Ca^{2+}]_{1/2}$ exhibited by the $cPLA_2$α-C2 domain in cells is the much higher local concentration of internal membranes, relative to the concentration of membranes used in the present *in vitro* study.

Effect of Total Lipid Concentration on the Ca^{2+} Dependence of C2 Domain Docking. All of the above experiments utilized total accessible lipid concentrations (100 μM) that were significantly lower than those estimated for the plasma membrane inner leaflet (400−800 μM) or for internal membranes (>3000 μM) in the cytoplasmic compartment of a living cell (*54*). In protein-to-membrane FRET studies, the maximum useful accessible lipid concentration is typically about 400 μM because of the excessive light scattering that occurs at higher concentrations. In order to establish the relationship between Ca^{2+}-sensitivity and lipid concentration, $[Ca^{2+}]_{1/2}$ values were measured for the docking of the PKCα-C2 domain to different concentrations of a PM mixture and for the docking of the $cPLA_2$α-C2 domain to

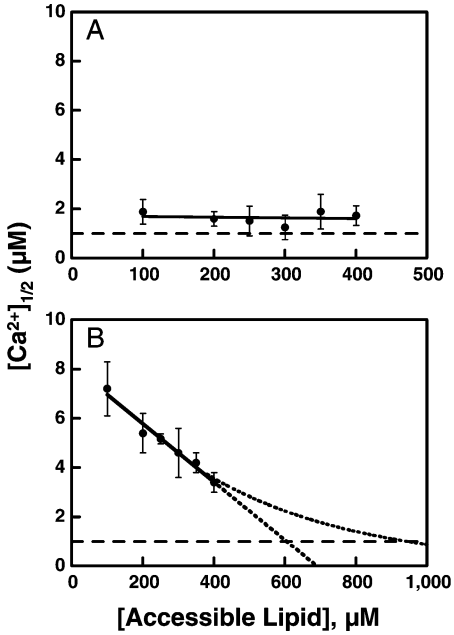

FIGURE 4: Effect of membrane concentration on the $[Ca^{2+}]_{1/2}$ value for Ca^{2+}-triggered docking of the PKCα- and $cPLA_2α$-C2 domains. Shown are the $[Ca^{2+}]_{1/2}$ values for the docking of C2 domains to sonicated unilamellar vesicles composed of physiological lipid mixtures. (A) $[Ca^{2+}]_{1/2}$ values for the docking of PKCα-C2 to the physiological mimic of the plasma membrane inner leaflet (Table 1, PM[2% PIP_2]) at different accessible lipid concentrations. The observed $[Ca^{2+}]_{1/2}$ value is independent of the lipid concentration in the range examined and is close to the threshold expected for a micromolar physiological Ca^{2+} signal (---). (B) $[Ca^{2+}]_{1/2}$ values for the docking of $cPLA_2α$-C2 to the physiological mimic of the internal membranes (Table 1, IM) at different accessible lipid concentrations. The observed $[Ca^{2+}]_{1/2}$ value is strongly dependent on the lipid concentration in the accessible range. Assuming the linear or asymptotic extrapolations shown (····), the $[Ca^{2+}]_{1/2}$ value would drop into the physiological micromolar range at a total lipid concentration between 700 and 1000 μM accessible lipid. Accessible lipid concentration was calculated as half of the total lipid concentration, assuming that approximately half of the lipid was exposed on the outer leaflet of the vesicles. The $[Ca^{2+}]_{1/2}$ values were determined by measuring the protein docking to the membrane during Ca^{2+} titrations as illustrated in Figures 2 and 3.

different concentrations of the IM mixture, as shown in Figure 4.

The $[Ca^{2+}]_{1/2}$ values shown in Figure 4A for the PKCα-C2 domain docking to a PM mixture (PM[2%PIP_2]) showed little change as the total accessible lipid concentration ranged from 100 μM up to 400 μM, where it approached cellular levels. Such findings are consistent with a model in which one or two Ca^{2+} ions bind initially to the free C2 domain, which then docks rapidly to the target membrane at all tested concentrations of the PM mixture (see Discussion). The limitations of the FRET assay prevented the determination of $[Ca^{2+}]_{1/2}$ for PKCα-C2 domain docking at IM lipid concentrations approaching those relevant in the cell (>3000 μM). However, the $[Ca^{2+}]_{1/2}$ measured for the docking of this C2 domain to a total accessible IM lipid concentration of 100 μM was 360 ± 80 μM (Figure 3A, Table 2), a value 300-fold higher than the Ca^{2+} concentration achieved during a micromolar cytoplasmic Ca^{2+} signal. Together, these findings indicate that the Ca^{2+} affinity of the PKCα-C2 domain is high enough to be activated by a physiological Ca^{2+} signal when the domain is in the vicinity of cellular concentrations of plasma membrane but not in the vicinity of internal membranes. Thus, the results obtained for the binding of the PKCα-C2 domain to complex lipid mixtures *in vitro* fully explain the observed specificity of this domain for the plasma membrane during micromolar cytoplasmic Ca^{2+} signals.

In contrast to the findings for the PKCα-C2 domain, the data presented in Figure 4B for the $cPLA_2α$-C2 domain reveal a strong dependence of $[Ca^{2+}]_{1/2}$ on the local concentration of the membranes. Notably, the $[Ca^{2+}]_{1/2}$ value for $cPLA_2α$-C2 docking to the IM mixture decreased linearly as the total accessible lipid concentration increased from 100 to 400 μM. Overall, $[Ca^{2+}]_{1/2}$ decreased over 2-fold from 7.2 ± 1.1 to 3.4 ± 0.4 μM over this range, representing a corresponding increase in Ca^{2+} affinity. Again, the limitations of the FRET assay prevented the extension of the experiment up to the intracellular concentration of total accessible internal membrane lipids (>3000 μM), but extrapolation of the data to these higher lipid concentrations (Figure 4B, dotted lines) suggests that $[Ca^{2+}]_{1/2}$ would enter the physiological micromolar range (Figure 4B, dashed line) at an accessible lipid concentration between 700 and 1000 μM. Assuming that such extrapolation is justified, the intracellular concentration of internal membranes is well above the level needed to generate efficient docking of the $cPLA_2α$-C2 domain during micromolar cytoplasmic Ca^{2+} signals. For comparison, the Ca^{2+} sensitivity of the $cPLA_2α$-C2 domain docking to a PM mixture (PM[2%PIP_2]) was also measured at an accessible lipid concentration of 400 μM, yielding a $[Ca^{2+}]_{1/2}$ value of 20 ± 2 μM. Together, these findings suggest that the Ca^{2+} affinity of the $cPLA_2α$-C2 domain is high enough to be activated by a physiological Ca^{2+} signal when the domain is in the vicinity of cellular concentrations of internal membranes but not in the vicinity of the plasma membrane, thereby explaining the specific targeting observed in living cells.

Overall, the present equilibrium binding data indicate that the Ca^{2+}-triggered intracellular targeting of PKCα- and $cPLA_2α$-C2 domains to plasma and internal membranes, respectively, can be fully explained by C2 domain interactions with target lipids. No interactions with other proteins appear to be needed for the inherent targeting specificities and sensitivities to micromolar Ca^{2+} signals exhibited by these two C2 domains. The plasma membrane specificity and micromolar Ca^{2+} activation of the PKCα-C2 domain in cells requires target lipids PS and PIP_2, which are found primarily on the inner leaflet of the plasma membrane. By contrast, the internal membrane specificity and micromolar Ca^{2+} activation of the $cPLA_2α$-C2 domain require the extremely high local concentration of PC generated by high internal membrane densities in the cell interior. For the latter C2 domain, a second target in addition to PC cannot be ruled out, although searches for such a second target lipid have been unsuccessful, supporting the conclusion that a high local concentration of PC is the only relevant target.

Kinetics of PKCα-C2 Domain Docking to Different Lipid Mixtures. In order to better define the molecular mechanisms underlying the targeting of C2 domains to specific membranes, the kinetics of membrane docking were investigated. Previous kinetic studies of membrane association and dissociation have been carried out for both PKCα- and $cPLA_2α$-C2 domains but only at super-physiological Ca^{2+} concentrations in the 100 to 1000 μM range (*10*, *12*, *23*, *45*). At

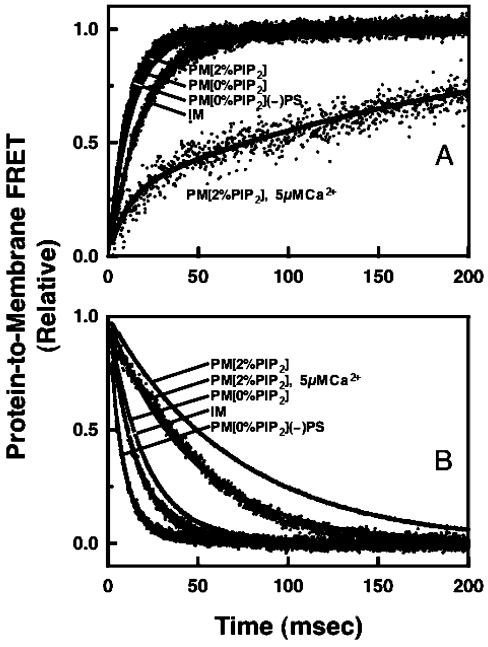

FIGURE 5: Kinetic analysis of PKCα-C2 domain docking to physiological lipid mixtures at different Ca^{2+} concentrations. (A) Association reaction triggered by the rapid mixing of membranes, 1 mM or 5 μM Ca^{2+}, and the C2 domain in a stopped-flow fluorimeter. The association kinetics observed at 1 mM Ca^{2+} were similar for the different plasma membrane ($PM[2\%PIP_2]$) and internal membrane (IM) mimics examined. By contrast, the association kinetics observed for the plasma membrane mimic ($PM[2\%PIP_2]$) at 5 μM Ca^{2+} exhibited a significantly slower second component in addition to the same fast component as that of the other reactions. (B) Dissociation reaction triggered by rapid mixing of the protein−Ca^{2+}−membrane complex with EDTA. The dissociation from the plasma membrane mimic ($PM[2\%PIP_2]$) was 5-fold slower than the dissociation from the internal membrane mimic (IM). Reducing the Ca^{2+} concentration from 1 mM to 5 μM had little effect. The solid curves underlying the data points represent the best fits with a single- or double-exponential process, yielding the apparent rate constants summarized in Table 4. Membrane association was quantitated by protein-to-membrane FRET measurements (legend for Figure 2).

these very high Ca^{2+} concentrations, the equilibrium binding data (Figure 2) indicate that the membrane specificity of the PKCα-C2 domain is weak such that the domain prefers target PM lipid mixtures but exhibits significant docking to nontarget IM mixtures as well. By contrast, at low Ca^{2+} concentrations, this domain exhibits strong specificity for its target PM lipid mixture. To pursue the molecular basis of these equilibrium results, membrane association and dissociation rates were measured for the PKCα-C2 domain binding to various lipid mixtures at different Ca^{2+} concentrations in a stopped-flow fluorescence spectrometer (see Materials and Methods). Association kinetics were measured by rapidly mixing a solution containing the C2 domain with a suspension of membranes, where both components were pre-equilibrated with the desired Ca^{2+} concentration before mixing. Dissociation kinetics were measured by mixing the preformed Ca^{2+}−protein−membrane complex with an EDTA solution. Following rapid mixing, the approach to equilibrium was monitored by protein-to-membrane FRET for both the association and dissociation reactions.

The kinetic results for the PKCα-C2 domain are shown in Figure 5 and Table 4. Strikingly, at a super-physiological Ca^{2+} concentration of 1 mM, the association kinetics were

Table 4: Kinetic Parameters for C2 Domain−Membrane Association and Dissociation

C2 domain	lipid mixture	$[Ca^{2+}]$ (μM)	k_{obs} (s^{-1})[a]	k_{off} (s^{-1})
PKCα-C2	$PM[6\%PIP_2]$	1000	66 ± 7	13 ± 1
	$PM[2\%PIP_2]$	1000	86 ± 10	14 ± 1
	$PM[6\%PIP_2](-)PS$	1000	58 ± 6	44 ± 3
	$PM[0\%PIP_2]$	1000	76 ± 8	48 ± 4
	$PM[0\%PIP_2](-)PS$	1000	94 ± 10*	116 ± 9
	IM	1000	50 ± 2*	62 ± 2
	$PM[2\%PIP_2]$	50	26 ± 1	21 ± 1
	$PM[0\%PIP_2]$	50	31 ± 2*	47 ± 2
	$PM[2\%PIP_2]$ (−)PS	50	19 ± 2*	51 ± 3
	$PM[2\%PIP_2]$	5	$61 \pm 9, 5 \pm 1$	18 ± 1
$cPLA_2$α-C2	IM	1000	22 ± 3	6 ± 1
	IM[13.5%PC]	1000	33 ± 4	15 ± 2
	$PM[6\%PIP_2]$	1000	30 ± 4	18 ± 2
	IM	50	17 ± 1*	8 ± 1
	$PM[2\%PIP_2]$	50	33 ± 1*	26 ± 2
	IM[13.5%PC]	10	17 ± 1*	15 ± 2
	$PM[2\%PIP_2]$	10	33 ± 1*	28 ± 3
	IM	5	9 ± 1*	7 ± 1

[a] The parameter k_{obs} is the exponential rate constant measured for the reversible association reaction under pseudo-first-order conditions. This reaction is an approach to equilibrium. In cases where the final equilibrium is dominated (>95%) by the bound state, k_{obs} is equivalent to k_{on} [L], where k_{on} is the second-order rate constant, and [L] is the constant target lipid concentration. In cases where the final equilibrium includes significant bound and free components, indicated by an asterisk, k_{obs} is equivalent to k_{on} [L] + k_{off} because the reverse reaction cannot be neglected.

nearly identical for PKCα-C2 domain docking to target ($PM[2\%PIP_2]$ or $PM[6\%PIP_2]$) and nontarget (IM, $PM[6\%PIP_2](-)PS$, or $PM[0\%PIP_2]$) membranes, varying no more than 1.7-fold. Similarly, although the kinetics of PKCα-C2 domain dissociation from different membranes were measurably different, the differences were too small to yield specific membrane docking. Thus, relative to the dissociation of the C2 domain from PM target membranes ($PM[2\%PIP_2]$ or $PM[6\%PIP_2]$), the removal PS or PIP_2 sped the dissociation 3- to 4-fold, whereas the simultaneous removal of both PS and PIP_2 sped the dissociation 8-fold, and the use of IM membranes sped the dissociation 5-fold. Overall, the moderate effects of lipid composition on the association and dissociation kinetics of the PKCα-C2 domain at 1 mM Ca^{2+} explains the measurable docking of this domain to nontarget membranes at this superphysiological Ca^{2+} concentration (Figure 3A). At the lower Ca^{2+} concentration of 5 μM, approaching the level of a micromolar Ca^{2+} signal, the poor equilibrium binding of the C2 domain prevented kinetic measurements for nontarget membranes. However, at this lower Ca^{2+} concentration, kinetic measurements were successfully carried out for the C2 domain docking to its PM target membrane. The association reaction revealed a new kinetic component exhibiting a rate constant 13- to 17-fold smaller than that previously observed at high Ca^{2+} concentrations. Such slow association can be attributed to the membrane docking of C2 domains that are only partially, rather than fully, occupied by Ca^{2+}. These observations support a mechanism (see Discussion) in which micromolar Ca^{2+} concentrations load the C2 domain with only one Ca^{2+} ion, which then docks to membranes in a reaction that exhibits a strong target specificity, in contrast to the weaker target specificity observed for the docking of the

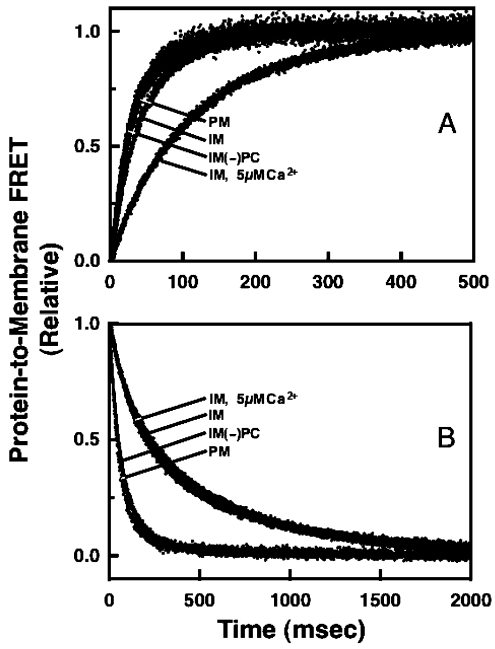

FIGURE 6: Kinetic analysis of the cPLA$_2$α-C2 domain docking to physiological lipid mixtures at different Ca^{2+} concentrations. (A) Association reaction triggered by the rapid mixing of membranes, 1 mM or 5 μM Ca^{2+}, and the C2 domain in a stopped-flow fluorimeter. The association kinetics observed at 1 mM Ca^{2+} were similar for the different internal membrane (IM) and plasma membrane (PM) mimics examined, but the kinetics were slowed when Ca^{2+} was reduced to 5 μM because of the decreased concentration of the free, Ca^{2+}-loaded C2 domain in the docking reaction (see text). (B) Dissociation reaction triggered by the rapid mixing of the protein−Ca^{2+}−membrane complex with EDTA. The dissociation from the internal membrane mimic (IM) was 3-fold slower than the dissociation from the plasma membrane mimic (PM-[6% PIP_2]). Reducing the Ca^{2+} concentration from 1 mM to 5 μM had little effect. The indicated abbreviations for membrane mimics correspond to the following lipid compositions in Tables 1 and 4: PM, PM[6%PIP_2]; IM, IM; IM(−)PC, IM[13.5%PC]. The solid curves underlying the data points represent the best fits with a single- or double-exponential process, yielding the apparent rate constants summarized in Table 4. Membrane association was quantitated by protein-to-membrane FRET measurements (legend for Figure 2).

domain loaded with two Ca^{2+} ions at super-physiological Ca^{2+} concentrations.

Kinetics of cPLA$_2$α-C2 Domain Docking to Different Lipid Mixtures. The kinetic results for the cPLA$_2$α-C2 domain are presented in Figure 6 and Table 4. At super-physiological Ca^{2+} concentrations of 1 mM or 50 μM, the association kinetics for C2 domain docking to target (IM) and nontarget (PM or IM with reduced PC levels) membranes were nearly identical, varying no more than 2.3-fold. The dissociation kinetics similarly varied no more than 4-fold among these different membranes. These findings explain the equilibrium binding results (Figure 3B) for the cPLA$_2$α-C2 domain at 1 mM Ca^{2+}, where the domain exhibited significant docking to both target and nontarget membranes at this super-physiological Ca^{2+} concentration (Figure 3B). When the Ca^{2+} concentration was reduced to the near physiological levels of 10 or 5 μM, sufficient equilibrium binding to both target and nontarget membranes was obtained to again carry out kinetic studies. Notably, the association kinetics still varied by no more than 5-fold between target (IM) and nontarget (PM or IM with reduced PC levels) membranes, whereas the dissociation kinetics varied only 4-fold. Such results explain the significant equilibrium binding of the cPLA$_2$α-C2 domain to nontarget membranes at these lower Ca^{2+} concentrations (Figure 3B). Finally, the observed rate constant for target (IM) membrane association remained nearly the same, within 2.4-fold when the Ca^{2+} concentration was reduced from 1 mM to 5 μM. It follows that the mechanism of Ca^{2+}-dependent membrane docking is essentially the same at both micromolar and super-physiological Ca^{2+} concentrations, indicating that for both of these conditions, Ca^{2+} activation is driven by the binding of two Ca^{2+} ions to the C2 domain prior to membrane docking, as previously described (*45*). Overall, the kinetic analysis of the cPLA$_2$α-C2 domain confirms the observation of the equilibrium analysis: this C2 domain exhibits significantly less discrimination between target and nontarget membranes than the PKCα-C2 domain.

DISCUSSION

Membrane-Specific Targeting of the PKCα- and cPLA$_2$-C2 Domains in Cells and in Vitro. The present studies of Ca^{2+}-stimulated intracellular targeting in the RAW macrophage cell line confirm the target membrane specificities previously observed for the PKCα- and cPLA$_2$α-C2 domains in other cell types (*12*, *13*, *27*, *46*, *57*). Upon Ca^{2+}-activation, the PKCα- and cPLA$_2$α-C2 domains specifically target to the plasma and internal membranes, respectively, with no detectable overlap in their targeting specificities. During typical intracellular Ca^{2+} signals, this remarkably specific targeting occurs as the Ca^{2+} concentration increases from a basal level of 0.1 μM up to a peak concentration of 0.5 to 0.9 μM in the bulk cytoplasm (*53*) and rarely exceeds 1 μM. The resulting findings for Ca^{2+}-triggered C2 domain docking to synthetic membrane vesicles significantly extend the current mechanistic understanding of specific C2 domain targeting at physiological Ca^{2+} concentrations. As predicted by previous models (*10*, *12*, *45*), the new results confirm that membrane specificity is dominated by C2 domain docking to the membrane lipids. Furthermore, these results clarify the lipid compositions and concentrations needed for such targeting specificity and shed light on the mechanism of targeting to specific membranes in the complex intracellular environment.

Two Types of Second Messenger-Induced Intracellular Targeting: MATA and TAMA. Two different mechanisms can be proposed for specific intracellular targeting arising from the coincidence detection of a global second messenger and a localized target molecule, such as the specific targeting of a C2 domain by coincidence detection of a global Ca^{2+} signal and localized target lipids. The messenger-activated-target-affinity (MATA) mechanism is characterized by a targeting protein that possesses an apo state with a high affinity for the second messenger and a low affinity for the target molecule. Specifically, in its apo state, the K_D for messenger binding is less than or approximately equal to the peak messenger concentration during the signal, whereas the K_D for target binding is significantly greater than the intracellular target concentration. In such a system, the binding of the second messenger activates the targeting protein by triggering a large increase in the affinity for the target molecule via their coupled binding equilibria. During a second messenger signaling event, the targeting protein will be activated everywhere because of its innate high

affinity for the messenger and will subsequently dock to all accessible target molecules. It follows that the targeting protein will be recruited to any and all regions of the cell where the global messenger signal extends and where accessible target molecules exist. This MATA mechanism is likely to be operating in second messenger pathways wherein the goal of activation is to drive docking to all available target molecules throughout the cell. However, this mechanism will only yield specific targeting when the target molecules are limited to specific locations within the cell.

The target-activated-messenger-affinity (TAMA) mechanism is quite different. This mechanism is characterized by a targeting protein that possesses an apo state with a low affinity for the second messenger as well as a low affinity for the target. Specifically, in its apo state, the K_D for messenger binding is significantly higher than the peak messenger concentration during the signal, and the K_D for target binding is significantly greater than the intracellular target concentration. During a second messenger signaling event, the affinity of the targeting protein is too low to bind the second messenger except in those regions of the cell where the local concentration of the target is high. In such regions, the high target concentration drives an increase in the effective affinity for the second messenger because of the thermodynamic effect of the coupled binding equilibrium. Thus, targeting proteins will be successfully activated and targeted by the second messenger only when they lie within a cellular region that both senses the second messenger signal and possesses a high local concentration of target molecules. This TAMA mechanism is useful in second messenger-activated pathways wherein the goal of activation is to drive docking only in regions of the cell possessing large pools of the target.

For the present C2 domains, TAMA is the logical mechanism because essential target lipids (PS and PC) are found in membranes throughout the cell but are significantly enriched in the target membranes (plasma and intracellular membranes). In the absence of target molecules, the PKCα and cPLA$_2$α C2 domains exhibit low Ca^{2+} affinities ($[Ca^{2+}]_{1/2}$ of 35 and 14 μM, respectively) (*10*, *23*, *45*) that would allow only minor activation by a physiological micromolar Ca^{2+} signal. For the PKCα C2 domain, the target lipid PS is found in significant concentrations in internal membranes (4 mol %) but is enriched in the inner leaflet of the plasma membrane (21 mol %) (*12*, *60*, *61*). For the cPLA$_2$α C2 domain, the target lipid PC is present at significant levels in the plasma membrane inner leaflet (10 mol %) but is substantially enriched in internal membranes (50 mol %) (*12*, *60*, *61*). Thus, for both of these C2 domains, TAMA is used to optimize the specificity of membrane targeting by limiting Ca^{2+} activation to the regions of the membrane containing the largest pools of common target lipids.

For conventional PKCα, β, and γ C2 domains, the TAMA mechanism is further enhanced by positive cooperativity in the binding of two or more PS molecules to the C2 domain (*23*) and by the exclusive plasma membrane localization of a second target lipid, PIP$_2$. During a Ca^{2+} signal, the combined TAMA effects of PS and PIP$_2$ enable conventional PKC C2 domains to drive highly specific Ca^{2+}-activated docking to the plasma membrane surface, where important protein substrates of the PKC kinase domain are located.

For the cPLA$_2$α C2 domain, it is not yet possible to rule out the existence of a second target lipid highly localized to the internal membranes (analogous to PIP$_2$ for PKC C2 domains) or the existence of a local, higher-than-bulk Ca^{2+} concentration in the vicinity of the target membrane. However, the present findings suggest that the high local density of PC found in internal membranes is essential to explain the observed specific targeting to these membranes during a Ca^{2+} signal. Because of extensive invagination and the dense packing of adjacent membrane structures, the local density of internal membranes in the cell interior is at least 10-fold higher than the membrane density in the vicinity of the plasma membrane (*54*). This high membrane density, together with the 5-fold higher mole percent of target PC found in internal membranes (*12*, *60*, *61*), ensures that the cPLA$_2$α C2 domain will experience at least a 50-fold higher local PC concentration in the vicinity of internal membranes relative to that of the plasma membrane. Such a large density of target lipid is proposed to drive TAMA targeting of the cPLA$_2$α C2 domain to internal membranes, thereby recruiting the associated phospholipase domain to these membranes, which possess the highest mole percent of the substrate arachidonate-containing phospholipids found anywhere in the cell.

In other types of Ca^{2+} signaling pathways, examples of both the MATA and TAMA mechanisms are evident. An interesting case is calmodulin, which possesses distinct N- and C-terminal domains, both of which are regulated by Ca^{2+} binding (*66*). This protein docks to a wide array of effector proteins using a diversity of different docking mechanisms (*67*, *68*). The K_D for Ca^{2+} binding to the C-terminal domain is in the low micromolar range (*69*), and this domain can dock independently to certain protein targets (*67*, *68*). Thus, the C-domain is an example of MATA targeting because a physiological Ca^{2+} signal substantially loads and activates the C-domain even in the absence of the target. By contrast, the K_D for Ca^{2+} binding to the N-terminal domain is in the tens of micromolar range (*69*) such that efficient Ca^{2+} activation of this domain requires the presence of target proteins that lower its effective Ca^{2+} K_D via the coupled binding equilibrium (*67*, *68*). Thus, calmodulin targeting events that require N-domain activation are best described by the TAMA mechanism. One advantage of this two-domain system is that it enables a single regulatory protein to utilize both the MATA and TAMA mechanisms, depending on which of its two domains is the limiting factor in target docking.

Molecular Mechanism of Ca^{2+}-Activated Membrane Docking by the PKCα-C2 Domain. The present studies of the PKCα-C2 domain show that the local densities of target lipids PS and PIP$_2$ on the inner leaflet of the plasma membrane are sufficient to drive Ca^{2+}-activated membrane docking during a physiological Ca^{2+} signal. At these micromolar Ca^{2+} levels, the data support a molecular mechanism in which the free C2 domain binds a single Ca^{2+} ion and then docks to PIP$_2$ on the membrane prior to associating with another Ca ion and PS. Equation 5 summarizes this multistep mechanism

$$C2 + Ca^{2+} \rightleftarrows C2\text{-}Ca^{2+}$$

$$C2\text{-}Ca^{2+} + PIP_2 \rightleftarrows C2^*\text{-}Ca^{2+}\text{-}PIP_2$$

$$C2^*\text{-}Ca^{2+}\text{-}PIP_2 + Ca^{2+} + PS_n \rightleftarrows C2^*\text{-}(Ca^{2+})_2\text{-}PIP_2\text{-}PS_n \quad (5)$$

where the target lipids PIP_2 and PS are located on the surface of the target membrane, and the asterisk indicates the membrane-bound protein. This proposed mechanism of specific PKCα-C2 domain docking is further strengthened by a molecular analysis of the individual binding steps. It has previously been shown that the empty C2 domain containing no bound Ca^{2+} ions cannot dock to the membrane because of the charge repulsion between the negative charges in the Ca^{2+} binding site and the negative surface charge of the membrane (*7*). The present model proposes that the binding of only one Ca^{2+} ion neutralizes enough of the protein negative charge to allow binding to PIP_2 on the membrane surface but not to PS, which is believed to require two Ca^{2+} ions for its association with the Ca^{2+} binding site (*7*, *19*). The binding of the C2 domain to PIP_2 would facilitate the subsequent binding of a second Ca^{2+} ion and one or more PS headgroups to the Ca^{2+} binding site. This mechanism explains the low Hill coefficient observed for Ca^{2+}-triggered docking to membranes containing PIP_2 because the binding of a single Ca^{2+} ion to one of the two Ca^{2+} binding sites would exhibit minimal positive cooperativity and thereby yield a Hill coefficient approaching 1.0, as observed (Table 2). The mechanism also explains the slow kinetic component observed in the membrane docking reaction at micromolar levels of activating Ca^{2+} (Table 4). The slow component is proposed to represent the docking of the singly Ca^{2+}-occupied C2 domain, which becomes undetectable at higher Ca^{2+} concentrations when the domain is loaded with two Ca^{2+} ions and docks more rapidly to the membrane. The model fully accounts for the synergistic effects of Ca^{2+}, PIP_2, and PS on membrane binding because high-affinity membrane docking is achieved only after the C2 domain, two Ca^{2+} ions, PIP_2, and at least one PS molecule form a stable complex. A key element of the model is the binding of the singly Ca^{2+}-occupied C2 domain to PIP_2 on the membrane surface, which greatly enhances the Ca^{2+} affinity of the second Ca^{2+} binding site because of the enhanced proximity to its PS ligand.

By contrast, physiological Ca^{2+} signals are unable to drive the docking of the PKCα-C2 domain to internal membranes. Because internal membranes lack accessible PIP_2 and have low mole fractions of PS relative to that of the plasma membrane, two Ca^{2+} ions must first bind to the C2 domain before it docks to PS on the membrane surface. However, the $[Ca^{2+}]_{1/2}$ value for the binding of two Ca^{2+} ions to the free PKCα-C2 domain is known to be 35 μM (*23*); thus, the intrinsic Ca^{2+} affinity is much lower than that needed for a physiological Ca^{2+} signal to drive activation and membrane docking in the vicinity of internal membranes. Instead, the equilibrium favors the unbound state of PKCα-C2 molecules located near internal membranes during a physiological Ca^{2+} signal. Thus, the ability of the singly Ca^{2+}-occupied PKCα-C2 domain to bind to PIP_2 explains the exquisite specificity of intracellular targeting to the cytosolic leaflet of the plasma membrane, where virtually all of the accessible PIP_2 is located and which contains high PS concentrations as well. For full length PKCα, the binding of C1 domain to diacylglycerol increases the lifetime of the bound state (*31*), and interactions with other proteins such as RACK also occur (*70*). Overall, however, the *in vitro* findings strongly suggest that the C2 domain interactions with PS and PIP_2 dominate plasma membrane targeting.

Molecular Mechanism of Ca^{2+}-Activated Membrane Docking by the $cPLA_2$-C2 Domain. The present results suggest that the specific targeting of the $cPLA_2$α-C2 domain to internal membranes is driven by the extremely high local density of the target lipid PC associated with these membranes. This high target concentration in the cell interior lowers the $[Ca^{2+}]_{1/2}$ value for membrane docking into the range accessible to cytosolic Ca^{2+} signals. The available evidence suggests a two-step molecular mechanism in which the free C2 domain binds two Ca^{2+} ions and then docks to membrane-bound PC as summarized in eq 6

$$C2 + 2\ Ca^{2+} \rightleftarrows C2\text{-}(Ca^{2+})_2$$

$$C2\text{-}(Ca^{2+})_2 + PC \rightleftarrows C2^*\text{-}(Ca^{2+})_2\text{-}PC \quad (6)$$

where the target lipid PC is located on a membrane surface, and the asterisk indicates the membrane-bound protein. This mechanism is supported by a molecular analysis of the microscopic docking events. Previous findings have shown that the empty C2 domain is initially prevented from membrane docking by its negatively charged Ca^{2+} binding site (*7*). During a Ca^{2+} signal, the domain binds two Ca^{2+} ions with positive cooperativity (*45*), which neutralize the charge of the Ca^{2+} binding site and allow the binding to the PC on the surface of internal membranes (*7*). In the absence of membranes, the free C2 domain exhibits a $[Ca^{2+}]_{1/2}$ value of 14 μM for the binding of two Ca^{2+} ions (*45*), but the high local concentration of PC in the cell interior pulls this binding equilibrium toward the membrane-docked state and decreases the effective $[Ca^{2+}]_{1/2}$ value, thereby approaching the micromolar range accessible to physiological Ca^{2+} signals. The high local concentration of PC needed to facilitate such Ca^{2+}-triggered docking is provied by the extremely dense, highly invaginated membrane distributions exhibited by the nuclear, Golgi, and ER, which all contain high mole fractions of PC (*54*). In contrast, physiological Ca^{2+} signals are unable to drive the binding of the domain to the plasma membrane, where the local concentration of PC is too low to bring the $[Ca^{2+}]_{1/2}$ value for membrane docking into the physiological range.

Conclusions. Overall, the target-activated-messenger-affinity (TAMA) mechanism is proposed to drive the highly specific intracellular targeting of the PKCα and $cPLA_2$α C2 domains purely on the basis of protein−lipid interactions. For each C2 domain, the $[Ca^{2+}]_{1/2}$ value for membrane docking varies with its location in the cell: when the C2 domain is far from its target membrane, the $[Ca^{2+}]_{1/2}$ value is too high for successful Ca^{2+} activation, but in the vicinity of the target membrane, high local concentrations of the target lipid decrease $[Ca^{2+}]_{1/2}$ into the range accessible to physiological Ca^{2+} signals. More broadly, the TAMA targeting mechanism and the distinct messenger-activated-target-affinity (MATA) mechanism are each expected to be utilized in different signaling pathways wherein targeting is controlled

both by a global second messenger and by one or more additional target ligands.

Finally, the present findings emphasize the importance of carrying out *in vitro* studies of signaling proteins at physiological ligand concentrations. In principle, super-physiological concentrations can drive interactions even when an important cofactor is missing, thereby slowing the identification of key cofactors. For many years, the importance of PIP_2 to the intracellular targeting of the PKCα-C2 domain to plasma membrane was obscured by *in vitro* studies (carried out in our laboratory and in others) using super-physiological concentrations of Ca^{2+} to drive membrane docking. At these Ca^{2+} concentrations, the C2 domain docks quite well to membranes lacking PIP_2. However, the present findings demonstrate that PIP_2 is essential for efficient membrane docking at physiological Ca^{2+} concentrations.

ACKNOWLEDGMENT

We thank Dr. Christina Leslie (National Jewish Medical and Research Center, Denver, CO) for the critical reading of this manuscript and for providing the construct expressing the cPLA$_2$α C2 domain. We also thank Dr. Jae-Won Soh (Inha University, Incheon, Korea) for providing the construct expressing the PKCα full length protein.

REFERENCES

1. Letunic, I., Copley, R. R., Schmidt, S., Ciccarelli, F. D., Doerks, T., Schultz, J., Ponting, C. P., and Bork, P. (2004) SMART 4.0: towards genomic data integration, *Nucleic Acids Res. 32*, D142−D144.
2. Nalefski, E. A., and Falke, J. J. (1996) The C2 domain calcium-binding motif: structural and functional diversity, *Protein Sci. 5*, 2375−2390.
3. Hurley, J. H. (2006) Membrane binding domains, *Biochim. Biophys. Acta 1761*, 805−811.
4. Cho, W., and Stahelin, R. V. (2006) Membrane binding and subcellular targeting of C2 domains, *Biochim. Biophys. Acta 1761*, 838−849.
5. Corbalan-Garcia, S., and Gomez-Fernandez, J. C. (2006) Protein kinase C regulatory domains: the art of decoding many different signals in membranes, *Biochim. Biophys. Acta 1761*, 633−654.
6. Benes, C. H., Wu, N., Elia, A. E., Dharia, T., Cantley, L. C., and Soltoff, S. P. (2005) The C2 domain of PKCdelta is a phosphotyrosine binding domain, *Cell 121*, 271−280.
7. Murray, D., and Honig, B. (2002) Electrostatic control of the membrane targeting of C2 domains, *Mol. Cell 9*, 145−154.
8. Hui, E., Bai, J., and Chapman, E. R. (2006) Ca2+-triggered simultaneous membrane penetration of the tandem C2-domains of synaptotagmin I, *Biophys. J. 91*, 1767−1777.
9. Davis, A. F., Bai, J., Fasshauer, D., Wolowick, M. J., Lewis, J. L., and Chapman, E. R. (1999) Kinetics of synaptotagmin responses to Ca2+ and assembly with the core SNARE complex onto membranes, *Neuron 24*, 363−376.
10. Nalefski, E. A., Wisner, M. A., Chen, J. Z., Sprang, S. R., Fukuda, M., Mikoshiba, K., and Falke, J. J. (2001) C2 domains from different Ca2+ signaling pathways display functional and mechanistic diversity, *Biochemistry 40*, 3089−3100.
11. Torrecillas, A., Corbalan-Garcia, S., and Gomez-Fernandez, J. C. (2003) Structural study of the C2 domains of the classical PKC isoenzymes using infrared spectroscopy and two-dimensional infrared correlation spectroscopy, *Biochemistry 42*, 11669−16681.
12. Stahelin, R. V., Rafter, J. D., Das, S., and Cho, W. (2003) The molecular basis of differential subcellular localization of C2 domains of protein kinase C-alpha and group IVa cytosolic phospholipase A2, *J. Biol. Chem. 278*, 12452−12460.
13. Evans, J. H., Gerber, S. H., Murray, D., and Leslie, C. C. (2004) The calcium binding loops of the cytosolic phospholipase A2 C2 domain specify targeting to Golgi and ER in live cells, *Mol. Biol. Cell 15*, 371−383.
14. Torrecillas, A., Laynez, J., Menendez, M., Corbalan-Garcia, S., and Gomez-Fernandez, J. C. (2004) Calorimetric study of the interaction of the C2 domains of classical protein kinase C isoenzymes with Ca2+ and phospholipids, *Biochemistry 43*, 11727−11739.
15. Perisic, O., Fong, S., Lynch, D. E., Bycroft, M., and Williams, R. L. (1998) Crystal structure of a calcium-phospholipid binding domain from cytosolic phospholipase A$_2$, *J. Biol. Chem. 273*, 1596−1604.
16. Sutton, R. B., and Sprang, S. R. (1998) Structure of the protein kinase Cbeta phospholipid-binding C2 domain complexed with Ca2+, *Structure 6*, 1395−13405.
17. Xu, G.-Y., McDonagh, T., Hsiang-Ai, Y., Nalefski, E. A., Clark, J. D., and Cumming, D. A. (1998) Solution structure and membrane interactions of the C2 domain of cytosolic phospholipase A$_2$, *J. Mol. Biol. 280*, 485−500.
18. Dessen, A., Tang, J., Schmidt, H., Stahl, M., Clark, J. D., Seehra, J., and Somers, W. S. (1999) Crystal structure of human cytosolic phospholipase A$_2$ reveals a novel topology and catalytic mechanism, *Cell 97*, 349−360.
19. Verdaguer, N., Corbalan-Garcia, S., Ochoa, W. F., Fita, I., and Gomez-Fernandez, J. C. (1999) Ca(2+) bridges the C2 membrane-binding domain of protein kinase Calpha directly to phosphatidylserine, *EMBO J. 18*, 6329−6338.
20. Nalefski, E. A., Sultzman, L. A., Martin, D. M., Kriz, R. W., Towler, P. S., Knopf, J. L., and Clark, J. D. (1994) Delineation of two functionally distinct domains of cytosolic phospholipase A$_2$, a regulatory Ca^{2+}-dependent lipid-binding domain and a Ca^{2+}-independent catalytic domain, *J. Biol. Chem. 269*, 18239−18249.
21. Edwards, A. S., and Newton, A. C. (1997) Regulation of protein kinase C βII by its C2 domain, *Biochemistry 36*, 15615−15623.
22. Newton, A. C. (2001) Protein kinase C: structural and spatial regulation by phosphorylation, cofactors, and macromolecular interactions, *Chem. Rev. 101*, 2353−2364.
23. Kohout, S. C., Corbalan-Garcia, S., Torrecillas, A., Gomez-Fernandez, J. C., and Falke, J. J. (2002) C2 domains of protein kinase C isoforms alpha, beta, and gamma: activation parameters and calcium stoichiometries of the membrane-bound state, *Biochemistry 41*, 11411−11424.
24. Corbalan-Garcia, S., Garcia-Garcia, J., Rodriguez-Alfaro, J. A., and Gomez-Fernandez, J. C. (2003) A new phosphatidylinositol 4,5-bisphosphate-binding site located in the C2 domain of protein kinase Calpha, *J. Biol. Chem. 278*, 4972−4980.
25. Rodriguez-Alfaro, J. A., Gomez-Fernandez, J. C., and Corbalan-Garcia, S. (2004) Role of the lysine-rich cluster of the C2 domain in the phosphatidylserine-dependent activation of PKCalpha, *J. Mol. Biol. 335*, 1117−1129.
26. Marin-Vicente, C., Gomez-Fernandez, J. C., and Corbalan-Garcia, S. (2005) The ATP-dependent membrane localization of protein kinase Calpha is regulated by Ca2+ influx and phosphatidylinositol 4,5-bisphosphate in differentiated PC12 cells, *Mol. Biol. Cell 16*, 2848−2861.
27. Evans, J. H., Murray, D., Leslie, C. C., and Falke, J. J. (2006) Specific translocation of protein kinase Calpha to the plasma membrane requires both Ca2+ and PIP2 recognition by its C2 domain, *Mol. Biol. Cell 17*, 56−66.
28. Sanchez-Bautista, S., Marin-Vicente, C., Gomez-Fernandez, J. C., and Corbalan-Garcia, S. (2006) The C2 Domain of PKCalpha is a Ca(2+)-dependent PtdIns(4,5)P(2) sensing domain: a new insight into an old pathway, *J. Mol. Biol. 362*, 901−914.
29. Kohout, S. C., Corbalan-Garcia, S., Gomez-Fernandez, J. C., and Falke, J. J. (2003) C2 domain of protein kinase calpha: elucidation of the membrane docking surface by site-directed fluorescence and spin labeling, *Biochemistry 42*, 1254−1265.
30. Malmberg, N. J., and Falke, J. J. (2005) Use of EPR power saturation to analyze the membrane-docking geometries of peripheral proteins: applications to C2 domains, *Annu. Rev. Biophys. Biomol. Struct. 34*, 71−90.
31. Oancea, E., and Meyer, T. (1998) Protein kinase C as a molecular machine for decoding calcium and diacylglycerol signals, *Cell 95*, 307−318.
32. Nalefski, E. A., and Newton, A. C. (2001) Membrane binding kinetics of protein kinase C betaII mediated by the C2 domain, *Biochemistry 40*, 13216−13229.
33. Allen, L. H., and Aderem, A. (1995) A role for MARCKS, the alpha isozyme of protein kinase C and myosin I in zymosan phagocytosis by macrophages, *J. Exp. Med. 182*, 829−840.
34. Mineo, C., Ying, Y. S., Chapline, C., Jaken, S., and Anderson, R. G. (1998) Targeting of protein kinase Calpha to caveolae, *J. Cell Biol. 141*, 601−610.

35. Rucci, N., Digiacinto, C., Orru, L., Millimaggi, D., Baron, R., and Teti, A. (2005) A novel protein kinase C {alpha}-dependent signal to ERK1/2 activated by {alpha}V{beta}3 integrin in osteoclasts and in Chinese hamster ovary (CHO) cells, *J. Cell. Sci. 118*, 3263−3275.
36. Cai, L., Holoweckyj, N., Schaller, M. D., and Bear, J. E. (2005) Phosphorylation of coronin 1B by protein kinase C regulates interaction with Arp2/3 and cell motility, *J Biol. Chem. 280*, 31913−31923.
37. McLaughlin, S., and Murray, D. (2005) Plasma membrane phosphoinositide organization by protein electrostatics, *Nature 438*, 605−611.
38. Levitan, I. B. (2006) Signaling protein complexes associated with neuronal ion channels, *Nat. Neurosci. 9*, 305−310.
39. Tao, J., Shumay, E., McLaughlin, S., Wang, H. Y., and Malbon, C. C. (2006) Regulation of AKAP-membrane interactions by calcium, *J. Biol. Chem. 281*, 23932−23944.
40. Newton, A. C. (1995) Protein kinase C. Seeing two domains, *Curr. Biol. 5*, 973−976.
41. Teruel, M. N., and Meyer, T. (2002) Parallel single-cell monitoring of receptor-triggered membrane translocation of a calcium-sensing protein module, *Science 295*, 1910−1912.
42. Bolsover, S. R., Gomez-Fernandez, J. C., and Corbalan-Garcia, S. (2003) Role of the Ca2+/phosphatidylserine binding region of the C2 domain in the translocation of protein kinase Calpha to the plasma membrane, *J. Biol. Chem. 278*, 10282−10290.
43. Alonso, F., Henson, P. M., and Leslie, C. C. (1986) A cytosolic phospholipase in human neutrophils that hydrolyzes arachidonoyl-containing phosphatidylcholine, *Biochim. Biophys. Acta 878*, 273−280.
44. Clark, J. D., Schievella, A. R., Nalefski, E. A., and Lin, L.-L. (1995) Cytosolic phospholipase A_2, *J. Lipid Mediators Cell Signalling 12*, 83−117.
45. Nalefski, E. A., Slazas, M. M., and Falke, J. J. (1997) Ca^{2+}-signaling cycle of a membrane-docking C2 domain, *Biochemistry 36*, 12011−12018.
46. Glover, S., de Carvalho, M. S., Bayburt, T., Jonas, M., Chi, E., Leslie, C. C., and Gelb, M. H. (1995) Translocation of the 85-kDa phospholipase A_2 from cytosol to the nuclear envelope in rat basophilic leukemia cells stimulated with calcium ionophore or IgE/antigen, *J. Biol. Chem. 270*, 15359−15367.
47. Perisic, O., Paterson, H. F., Mosedale, G., Lara-González, S., and Williams, R. L. (1999) Mapping the phospholipid-binding surface and translocation determinants of the C2 domain from cytosolic phospholipase A_2, *J. Biol. Chem. 274*, 14979−14987.
48. Nalefski, E. A., and Falke, J. J. (1998) Location of the membrane-docking face on the Ca^{2+}-activated C2 domain of cytosolic phospholipase A_2, *Biochemistry 37*, 17642−17650.
49. Frazier, A. A., Wisner, M. A., Malmberg, N. J., Victor, K. G., Fanucci, G. E., Nalefski, E. A., Falke, J. J., and Cafiso, D. S. (2002) Membrane orientation and position of the C2 domain from cPLA2 by site-directed spin labeling. (The erratum appears in *Biochemistry* (2002) Jun 11, *41*, 7528.), *Biochemistry 41*, 6282−6292.
50. Malmberg, N. J., Van Buskirk, D. R., and Falke, J. J. (2003) Membrane-docking loops of the cPLA2 C2 domain: detailed structural analysis of the protein-membrane interface via site-directed spin-labeling, *Biochemistry 42*, 13227−13240.
51. Evans, J. H., and Leslie, C. C. (2004) The cytosolic phospholipase A2 catalytic domain modulates association and residence time at Golgi membranes, *J. Biol. Chem. 279*, 6005−6016.
52. Nalefski, E. A., McDonagh, T., Somers, W., Seehra, J., Falke, J. J., and Clark, J. D. (1998) Independent folding and ligand specificity of the C2 calcium-dependent lipid binding domain of cytosolic phospholipase A_2, *J. Biol. Chem. 273*, 1365−1372.
53. Berridge, M. J. (1993) Inositol trisphosphate and calcium signalling, *Nature 361*, 315−325.
54. Griffiths, G., Warren, G., Quinn, P., Mathieu-Costello, O., and Hoppeler, H. (1984) Density of newly synthesized plasma membrane proteins in intracellular membranes. I. Stereological studies, *J. Cell Biol. 98*, 2133−2141.
55. Laemmli, U. K. (1970) Cleavage of structural proteins during the assembly of the head of bacteriophage T4, *Nature 227*, 680−685.
56. Copeland, R. A. (1994) *Methods for Protein Analysis: A Practical Guide to Laboratory Protocols*, Chapman and Hall, New York.
57. Corbalan-Garcia, S., Rodríguez-Alfaro, J. A., and Gómez-Fernández, J. C. (1999) Determination of the calcium-binding sites of the C2 domain of protein kinase Cα that are critical for its translocation to the plasma membrane, *Biochem. J. 337*, 513−521.
58. Evans, J. H., Spencer, D. M., Zweifach, A., and Leslie, C. C. (2001) Intracellular calcium signals regulating cytosolic phospholipase A2 translocation to internal membranes, *J. Biol. Chem. 276*, 30150−30160.
59. Hirabayashi, T., Kume, K., Hirose, K., Yokomizo, T., Iino, M., Itoh, H., and Shimizu, T. (1999) Critical duration of intracellular Ca^{2+} response required for continuous translocation and activation of cytosolic phospholipase A_2, *J. Biol. Chem. 274*, 5163−5169.
60. van Meer, G. (1998) Lipids of the Golgi membrane, *Trends Cell Biol. 8*, 29−33.
61. Vance, D. E., and Vance, J. E. (2002), *Biochemistry of Lipids, Lipoproteins, and Membranes*, Elsevier Science, Burlington, MA.
62. Hope, H. R., and Pike, L. J. (1996) Phosphoinositides and phosphoinositide-utilizing enzymes in detergent-insoluble lipid domains, *Mol. Biol. Cell 7*, 843−51.
63. Laux, T., Fukami, K., Thelen, M., Golub, T., Frey, D., and Caroni, P. (2000) GAP43, MARCKS, and CAP23 modulate PI(4,5)P(2) at plasmalemmal rafts, and regulate cell cortex actin dynamics through a common mechanism, *J. Cell Biol. 149*, 1455−1472.
64. Caroni, P. (2001) New EMBO members' review: actin cytoskeleton regulation through modulation of PI(4,5)P(2) rafts, *EMBO. J. 20*, 4332−4336.
65. Golub, T., and Caroni, P. (2005) PI(4,5)P2-dependent microdomain assemblies capture microtubules to promote and control leading edge motility, *J. Cell Biol. 169*, 151−165.
66. VanScyoc, W. S., Sorensen, B. R., Rusinova, E., Laws, W. R., Ross, J. B., and Shea, M. A. (2002) Calcium binding to calmodulin mutants monitored by domain-specific intrinsic phenylalanine and tyrosine fluorescence, *Biophys J. 83*, 2767−2780.
67. Vetter, S. W., and Leclerc, E. (2003) Novel aspects of calmodulin target recognition and activation, *Eur. J. Biochem. 270*, 404−414.
68. Ishida, H., and Vogel, H. J. (2006) Protein-peptide interaction studies demonstrate the versatility of calmodulin target protein binding, *Protein Pept. Lett. 13*, 455−465.
69. Peersen, O. B., Madsen, T. S., and Falke, J. J. (1997) Intermolecular tuning of calmodulin by target peptides and proteins: differential effects on Ca2+ binding and implications for kinase activation, *Protein Sci. 6*, 794−807.
70. Ron, D., Luo, J., and Mochly-Rosen, D. (1995) C2 region-derived peptides inhibit translocation and function of β protein kinase C *in vivo J. Biol. Chem. 270*, 24180−24187.

BI062140C